DEMOCRATIC AND POPULAR REPUBLIC OF ALGERIA MINISTRY OF HIGHER EDUCATION AND SCIENTIFIC RESEARCH
MOHAMED BOUDIAF UNIVERSITY - M'SILA

FACULTY OF SCIENCES
PHYSICS DEPARTMENT
N° : PH/MAT/03/2024

DOMAIN: MATTERIAL SCIENCES
SECTOR: PHYSICS
OPTION: MATERIAL PHYSICS

Thesis presented for obtaining the Academic Master's degree

By: Bouchelaleg Nadia and Benseidi Zoubida

Title

Adequate physical properties of the double cubic perovskite-type using first principal calculation

Defended before the jury composed of: 15/05/2024

Salmi Mohamed	University of M'sila	Chairman
Ghebouli Mohamed Amine	University of M'sila	Supervisor
Bouferrache Karim	University of M'sila	Examiner

2023 /2024

DEDICATION:

I DEDICATE THIS MODEST WORK

TO MY FATHER FOR EVERYTHING HE GAVE ME.

TO MY MOTHER FOR ALL HER SACRIFICE.

TO MY HUSBAND

TO MY SON

TO MY BROTHERS AND SISTERS.

TO THE WHOLE FAMILY.

TO ALL MY FRIENDS.

TO ALL THOSE WHO CONTRIBUTED DIRECTLY OR INDIRECTLY TO THIS WORK.

BOUCHELALEG NADIA

Dedication:

I dedicate this modest work

To my deceased father, may God have mercy on him.

To my mother for all her sacrifice.

To my kids

To my brothers and sisters.

To the whole BENSEIDI family.

To all my friends.

To all those who contributed directly or indirectly to this work.

BENSEIDI ZOUBIDA

Acknowledgments:

I thank above all ALLAH the Almighty who gave me will, patience and health, allowing me to complete this present work.

I would first like to express my deepest thanks to my supervisor ***Ghebouli Mohamed Amine****, for his wise advice both on the treatment of my dissertation subject and on the "sidelines", scientific and human. The rigor that guided his supervision as well as the long time spent correcting and discussing the publication projects, and above all, this thesis manuscript were truly appreciated.*

I would like to express my best wishes for him and his entire family.

I warmly thank Professor ***Salmi Mohamed*** *for agreeing to chair the jury for my dissertation defense.*

I am very grateful to ***Mr. Bouferrache Karim****, for agreeing to examine my research work.*

My thanks also go to all colleagues in the physics department at the University of M'sila.

A big thank you to all my family who have always been there when I needed them.

Contents Table

CHAPTER I : SEMICONDUCTOR

CHAPTER II : AB-INITIO METHODS AND SIMULATION TOOL

CHAPTER III: RESULTS AND DISCUSSION

Figure List

Table List

GENERAL

INTRODUCTION

General Introduction

Due to the needs of industrial development and the growth of the world population, energy consumption has increased rapidly in recent decades. Today, a large part of the world uses fossil or "non-renewable" fuels (oil, natural gas, coal).

These energies are considered exhausted resources. Therefore, we must look for other alternatives to produce this energy. In addition to their exhaustible nature, fossil resources pose disadvantages such as global warming with greenhouse gas emissions, radioactive pollution, CO2 emissions, etc.

For these reasons the world uses renewable energies such as hydroelectric energy, wind energy, biomass energy, geothermal energy, photovoltaic solar energy. These renewable energies are of natural origin, inexhaustible and non-polluting.

Photovoltaic energy comes from the conversion of sunlight into electricity. This conversion occurs within semiconductor materials, which have the property of releasing charge carriers (electrons and holes) under the influence of external excitation. Standard photovoltaic cells placed on the market have an electrical efficiency of around 17%.

The semiconductors used in the manufacture of solar cells are the subject of much research. First generation cells based on material consisting of a silicon wafer occupy an important place. The production method is very expensive, research has focused on the use of thin film technology.

This technique plays a considerable role in reducing the cost of cell manufacturing. In this generation, the most common method is based on chalcogenides. These materials are promising because of their large absorption coefficient and their optimal gap for photovoltaic conversion.

Our work consists of understanding the behaviors of the structural, electronic and optical properties of Cs_2MCl_6 (M = Si , Sn, Ge and Pb) semiconductors.

Then, we propose new solar cell structures based on Cs_2SiCl_6 and to Cs_2GeCl_6 reduce the cost and improve the performance. This work has two parts, where we study the structural, electronic and optical properties of Cs_2MCl_6 (M = Si , Sn, Ge and Pb) semiconductors with the wien2k code. We verify that the properties cited above are adequate.

The second part is devoted to the digital simulation of a new solar cell structure based on Cs_2SiCl_6 and to Cs_2GeCl_6 semiconductors, using the **COMSOL** simulator. The aim is to improve electrical characteristics (the electrical current) of solar cell.

CHAPTER I

SEMICONDUCTOR

I.1. Introduction

The solar cell is a semiconductor component that converts incident illumination into electrical energy. The phenomenon involved, the photoelectric effect, consists of the appearance of a potential difference produced by the generation of charge carriers by light excitation in the vicinity of a junction.

The solar cell is a PN junction whose operation is based on the absorption of solar light flux, the generation and collection of charges. In this chapter we present general information on semiconductors, the operating principle of photovoltaic cells and the different technological paths.

I. 2. History of photovoltaic cells

In 1839 the photovoltaic effect was discovered by observing the electrical behavior of electrons in a liquid. He concludes that if a material is exposed to sufficient solar radiation, the electrons generate a direct electric current which translates the photovoltaic effect and photovoltaic energy.

In 1875, Werner Von Siemens published an article on the photovoltaic effect in semiconductors. William filed his patent in 1913 which showed that the photovoltaic cell converted solar energy into electrical energy. Robert Millikan's work confirms the study of Albert Einstein (done in 1905) in 1916 and was the first to produce direct current electricity with a photovoltaic cell. Photovoltaic panels are taking a big step forward thanks to the oil crisis and the search for energy for satellites. In 1954, American researchers Chapin, Pearson and Prince developed a photovoltaic cell with an efficiency of around 6%, and in 1958 it reached around 9%. In 1973, the University of Delaware powered the first house with photovoltaic cells and installed the panels (set of cells) in this house. After all these advances, it was only between 1995 and 2001 that photovoltaic panels were commercialized [1]. We schematize the evolution of photovoltaic cells in Fig. I 1.

I. 3. Definition of a semiconductor

A semiconductor is a material whose electrical conductivity is intermediate between that of conductors (~) and insulators (~). This conductivity varies under the effect of temperature, illumination and the presence of impurities (doping, crystal defects) [2, 3]. The electrical conductivity at room temperature of insulators, semiconductors and conductors is shown schematically on the Fig. I 2.

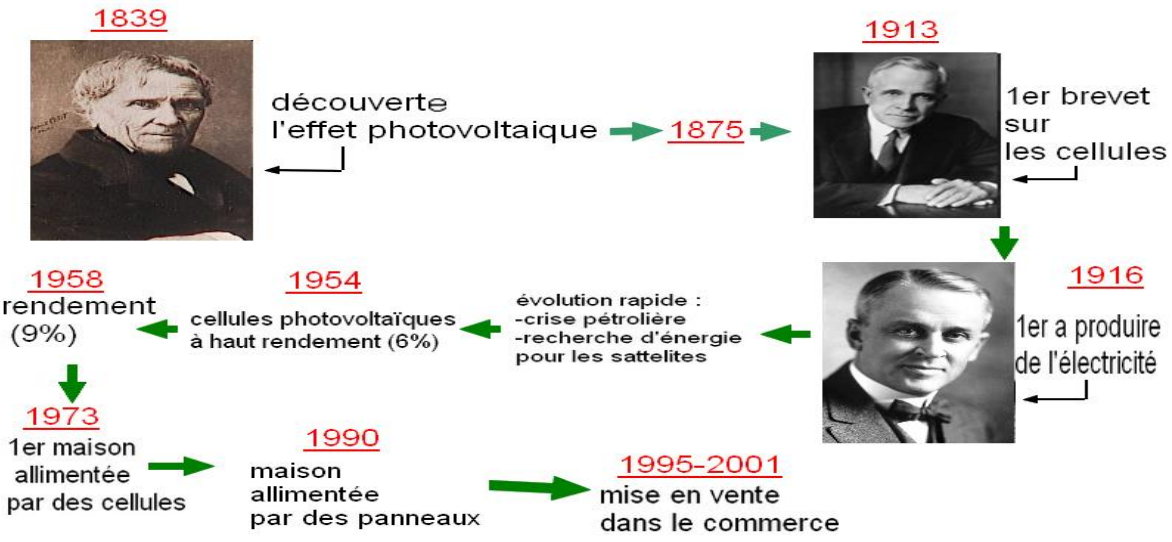

Fig. I. 1. Evolution diagram of photovoltaic cells.

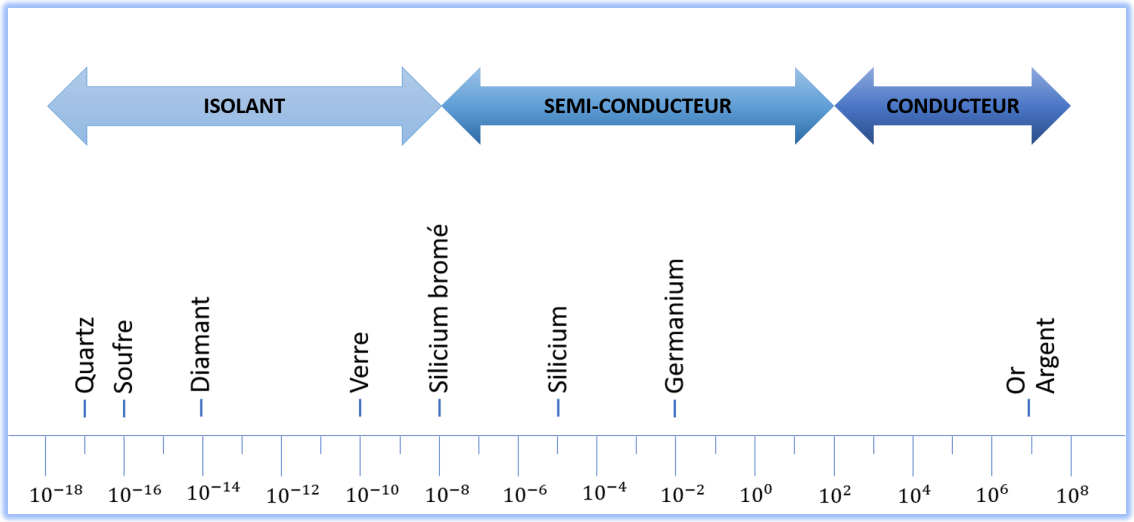

Fig. I. 2. Electrical conductivity at room temperature of different materials.

I. 4. Semiconductor type

There are two types of semiconductors, one perfect called intrinsic and the other doped called extrinsic.

I. 4. 1. Pure or intrinsic semiconductor

A pure semiconductor, perfectly regular, without structural defects and containing no impurities is called intrinsic. Its electrical behavior depends solely on its structure and thermal excitation. It has the following characteristics:

- Charge carriers (electrons) are created by crystal defects and by thermal excitation of electrons in the valence band.

- The number of electrons in the conduction band is equal to the number of holes in the valence band.
- The intrinsic Fermi level EF is found near the center of the band gap.
- The intrinsic concentration of the carriers and the intrinsic Fermi level are calculated by the following expressions [1]:

The calculation of the intrinsic concentration of carriers and the intrinsic Fermi level requires the introduction of the notion of energy density of states $N(E)$. This density, a function of the electronic energy E, corresponds to the space available for electrons in the conduction band $N_C(E)$ and to the space available for holes in the valence band. $N_V(E)$

$$\begin{cases} N_C(E) = \dfrac{1}{2\pi^2}\left(\dfrac{2m_c}{\hbar^2}\right)^{3/2}\sqrt{E-E_c} \\ N_V(E) = \dfrac{1}{2\pi^2}\left(\dfrac{2m_c}{\hbar^2}\right)^{3/2}\sqrt{E_v-E} \end{cases} \qquad (I.1)$$

With $\hbar$, m_c et m_v are respectively the normalized Planck constant, the effective mass of density of states in the conduction band and that in the valence band.

The effective number of electrons and holes, in each of the bands, requires knowledge of the probability of the presence of an electron on an energy level E. This probability is given by the Fermi-Dirac function [2]:

$$f(E) = \frac{1}{1+e^{(E-E_F)/k_BT}} \qquad (I.2)$$

With k_B, T et E_F are respectively the Boltzmann constant, the temperature and the Fermi energy.

Electron density *n* (holes *p*) in the conduction band (valence) is then obtained by the expression [2]:

$$\begin{cases} n = \int_{E_c}^{\infty} N_C(E)\, f(E)\, dE \\ p = \int_{-\infty}^{E_v} N_V(E)\left[1-f(E)\right] dE \end{cases} \qquad (I.3)$$

The Fermi function can be simplified into exponential form, which leads to:

$$\begin{cases} n = N_C e^{-\frac{E_C-E_F}{k_BT}} \\ p = N_V e^{\frac{E_v-E_F}{k_BT}} \end{cases} \qquad (I.4)$$

with N_c et N_v are respectively the effective density of electrons in the conduction band and that of holes in the valence band. We define the intrinsic carrier density by the relation:

$$n_i = \sqrt{n \cdot p} = \sqrt{N_c N_v} e^{\frac{E_v - E_c}{2kT}} \qquad (I.5)$$

In the case where there is equality of carrier densities for an intrinsic semiconductor, the energy of the Fermi level is given by:

$$E_F = \frac{1}{2}(E_c + E_v) + \frac{1}{2} kT \ln \frac{N_V}{N_C} \qquad (I.6)$$

Notice:

Intrinsic semiconductors are purely theoretical, because no current technique makes it possible to manufacture perfectly regular and perfectly monatomic crystals and the fact that they have very low conductivity, unless brought to very very high temperatures, makes them not interesting. Therefore, studies are moving towards extrinsic semiconductors.

I. 4. 2. Doped or extrinsic semiconductor

An extrinsic semiconductor is an intrinsic semiconductor doped with specific impurities giving it electrical properties adapted to the field of use of this material. The introduction of these dopants disrupts the forbidden bands, creating accessible states inside these bands and making the gap more permeable. Depending on the type of doping, two types of semiconductors are distinguished:

I. 4. 2. 1. N-type extrinsic semiconductor

An N-doped or N-type semiconductor is a semiconductor into which donor-type impurities (N, P, As, Sb) are introduced, which can transfer an electron to the conduction band, to make a bond with the semiconductor crystal. A typical example is the doping of Si by donor atoms of column V (As for example) which will present four covalent bonds and one free electron (Fig. I.3).

This electron weakly bound to the atom can be excited towards the conduction band. This excitation does not lead to the formation of holes in this type of material and the number of electrons exceeds that of the holes. Electrons and holes are the majority and minority carriers, respectively.

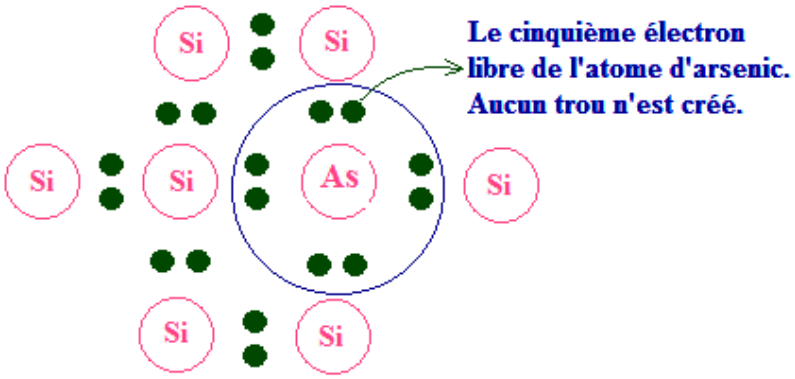

Fig. I. 3. Representative diagram of the silicon semiconductor N doped with arsenic impurities.

I. 4. 1. 2. P-type extrinsic semiconductor

A P-type semiconductor is an intrinsic semiconductor where acceptor-type impurities (B, Al, Ga, In) have been introduced. These dopants acquire an electron from the conduction band to make a bond with the semiconductor crystal, thus creating an excess of holes. P-type doping therefore consists of increasing the hole density in the intrinsic semiconductor.

In the case of silicon, we include a trivalent atom which forms three covalent bonds and creates a hole in the structure. Holes and electrons are the majority and minority carriers, respectively. Fig. I.2 shows a representative diagram of a P-doped semiconductor with phosphorus impurities.

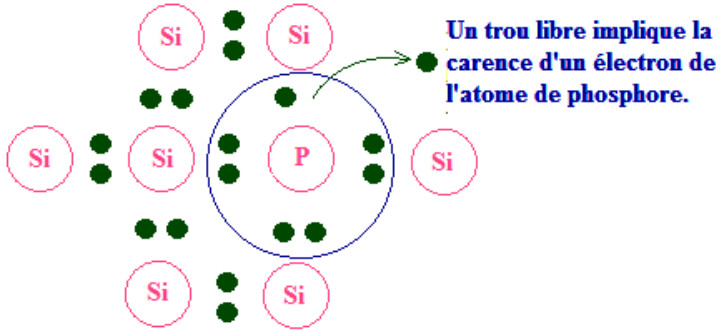

Fig. I. 4. Representative diagram of the Si semiconductor P doped with phosphorus impurities.

I. 4. 3. Semiconductor classification

Semiconductors are classified into groups of atoms which compose them according to their characteristics and according to their chemical composition. The Roman numerals (I, II, III, IV, V, VI etc.) refer to the columns of the periodic table of elements.

The most common elementary semiconductors are silicon (Si), germanium (Ge) and gray tin (α-Sn) belonging to group IV of the Mendeleev periodic table.

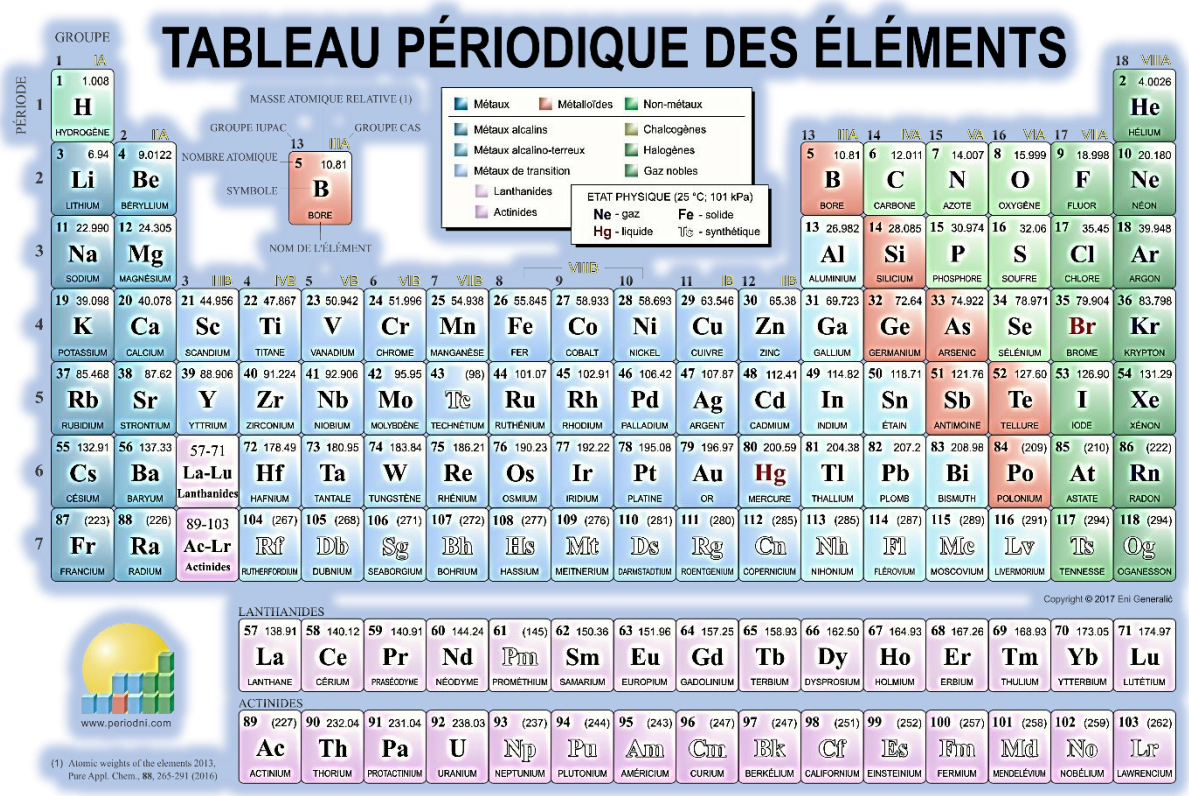

Fig. I. 5. Mendeleev's periodic table.

Group II includes the following elements: Be, Mg, Ca, Sr and Ba; those of group III are N, P, As and Sb, B, Al, Ga, In belong to group V while O, S, Se and Te form group VI (**Fig.I.5**). The alloy of semiconductor elements from two different groups gives a binary semiconductor whose properties are intermediate and the combination of three or four elements from these groups gives a ternary or quaternary alloy whose interest depends on the properties that he introduces.

I. 5. Semiconductor groups

I.5.1. Simple semiconductors

A simple semiconductor is made up of a single element such as the semiconductor of column IV of the periodic table such as silicon (Si) and germanium (Ge) [4].

I.5.2. II-VI Semiconductors

Binary semiconductors of class (IIVI) consist of one element from column II and another from column VI of the periodic table. Zinc oxide is mentioned (ZnO), Cadmium sulfide (CdS), Zinc sulfide (ZnS), Zinc selenide (ZnSe), Zinc telluride (ZnTe), Cadmium selenide (CdSe) [4].

I.5.3. IIIV Semiconductors

A IIIV semiconductor is a composite made from elements from column III of the periodic table (boron, aluminum, gallium, indium, etc.), and elements from column V (nitrogen, phosphorus, arsenic, antimony, etc. .). IIIV semiconductors are of great interest due to their properties:

1- They are robust.

2- They have high thermal conductivity.

3- Their melting point is high.

4- They have a direct bandgap.

These materials are used in microelectronics in integrated circuits, in photovoltaic cells and in optoelectronic devices such as light-emitting diodes (LEDs or LEDs in English). These types of semiconductors are shown in Fig. I. 6.

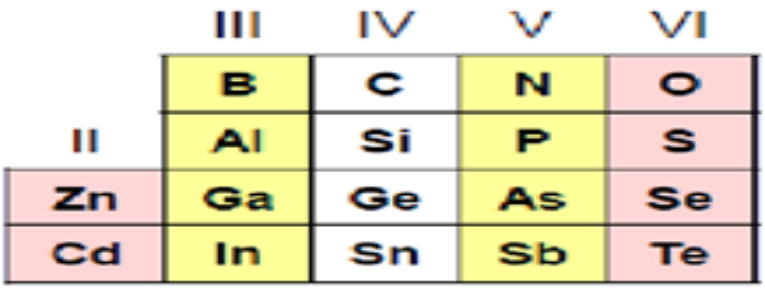

Fig. I. 6. The different types of semiconductors.

I. 5. 4. Binary and ternary semiconductor compounds

Certain compounds formed from elements III and V exhibit semiconductor properties. We also note semiconductors II and VI. This category of compound is made up of at least two different types of atoms.

There are ternary semiconductors formed by elements belonging to three different groups. Compounds including boron and aluminum are of interest in the electronics[5] and optoelectronics[6] fields.

I. 6. Crystal structure

Condensed matter takes on a solid state which depends on its formation. We distinguish the amorphous state, where the arrangement of atoms is random. A crystallized state is characterized by a periodic arrangement of atoms. We note the zinc blende and hexagonal structures.

I.6.1. Crystal lattice

Crystalline solids are characterized by a periodic arrangement of atoms along the three directions of space called a crystal lattice. There are 14 types of crystal lattices called Brallais lattices. Examples include the centered cubic (CC), face-centered cubic (CFC), compact hexagonal (HC) and diamond lattices [7].

I. 6. 2. Reciprocal network

In crystallography, the reciprocal lattice of a Brallais lattice is the set of vectors K such that: eiKR =1, K is a vector of the reciprocal lattice and R is a translation vector of the direct lattice.

I. 6. 3. Brillouin zone

The electron wave functions and the corresponding energies depend on the wave vector of the electron. The energy band structure of the semiconductor is represented in the reciprocal space and in the different directions of the wave vectors.

The reciprocal network, associated with the zinc blende structure is shown in Fig. I. 7. The unit cell of the zinc blende structure corresponds to the first Brillouin zone, which has the shape of an octahedron truncated by the six faces of a cube. It has a center of symmetry at the origin Γ. The Brillouin zone is a primitive unit cell of the reciprocal lattice of fundamental importance for the study of the electronic properties of crystals, particularly in semiconductors [8, 9].

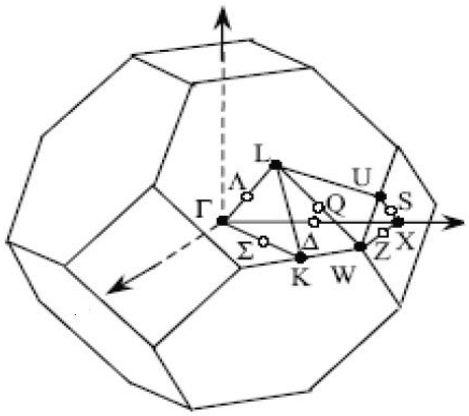

Fig. I. 7. First Brillouin zone of a zinc blende structure.

I. 7. Mesh Settings

The mesh parameters mean the dimensions of the elementary cell of the crystal lattice [10]. In the most complex case, which is the triclinic network, we have 6 parameters: three dimensions *a*, *b* and *c*, and three angles alpha, beta and gamma. In the case of the cubic network, we only

cite one mesh parameter, a (since $a = b = c$ et $\alpha = \beta = \gamma = 90°$). As our study is based on perovskite compounds that crystallize in a $Pm\bar{3}m$ (#221) symmetry group structure, this crystal lattice is simple cubic whose base cell consists of atoms A, B and F at positions A (0 , 0, 0), B (1/2, 1/2, 1/2) and F (0.5, 0.5, 0), F (0.5, 0, 0.5) and F (0, 0.5, 0.5).

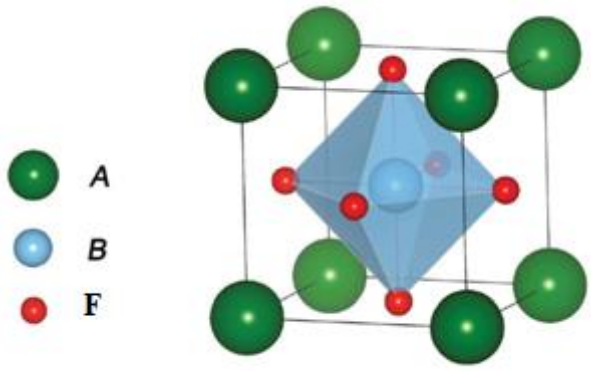

Fig. I. 8. Conventional mesh of the ABF_3 type perovskite structure [11].

I. 8. Mechanical properties

Mechanical properties represent the reaction of materials to external stress applications such as compression, traction, shear, etc. They essentially depend on the bonding forces that exist between the atoms constituting the material.

I. 8.1. Elastic constants

Elastic constants reflect the disposition of a material to deform in response to a given stress. In general, an anisotropic material deforms if a stress σ is applied to it. Within the limits of elasticity, this deformation ε is proportional to the stress applied to it.

According to the method developed by Nielson and Martin [12], the generalized Hooke's law shows that the components of the stress tensor σ_{ij} are linear functions of the components of the strain tensor ε_{kl}, where the constant of proportionality defines the tensor elastic constants C_{ijkl}.

In the case of the cubic structure, the number of elastic constants is reduced to three independent constants C_{11} , C_{12} and C_{44} and by symmetry, Hooke's law is written [13, 14]:

$$\sigma_{ij} = \sum_{ijkl} C_{ijkl}\varepsilon_{kl} \qquad (I.7)$$

Thus, the constraint tensor is given by:

$$[\sigma_{ij}] = \begin{bmatrix} \sigma_{11} & \sigma_{12} & \sigma_{13} \\ \sigma_{21} & \sigma_{22} & \sigma_{23} \\ \sigma_{31} & \sigma_{32} & \sigma_{33} \end{bmatrix} \qquad (I.8)$$

The deformation tensor is:

$$[\varepsilon_{kl}] = \begin{bmatrix} \varepsilon_{11} & \varepsilon_{12} & \varepsilon_{13} \\ \varepsilon_{21} & \varepsilon_{22} & \varepsilon_{23} \\ \varepsilon_{31} & \varepsilon_{32} & \varepsilon_{33} \end{bmatrix} \quad (I.9)$$

In the case of materials with cubic symmetry, the elastic constant tensor is written:

$$[C_{ijkl}] = \begin{bmatrix} C_{11} & C_{12} & C_{12} & 0 & 0 & 0 \\ C_{12} & C_{11} & C_{12} & 0 & 0 & 0 \\ C_{12} & C_{12} & C_{11} & 0 & 0 & 0 \\ 0 & 0 & 0 & C_{44} & 0 & 0 \\ 0 & 0 & 0 & 0 & C_{44} & 0 \\ 0 & 0 & 0 & 0 & 0 & C_{44} \end{bmatrix} \quad (I.10)$$

We distinguish two rigidity constants C_{11} and C_{12} and a shear constant C_{44} given by:

$$C_{44} = \frac{1}{2}(C_{11} - C_{12}) \quad (I.11)$$

The elastic constants C_{12} and C_{44} essentially act on the shape. The combination of C_{12} with C_{11} gives the compressibility modulus and the shear modulus. These elastic constants are expressed as a function of the Lamé coefficients λ and μ by the relations [15, 16]:

$$C_{11} = \lambda + 2\mu \ , \ C_{12} = \lambda \ \text{ et } \ C_{44} = \mu \quad (I.12)$$

I. 8. 2. Anisotropy factor

Anisotropy is the property of a physical quantity to be direction dependent. It is expressed by a factor called anisotropy factor defined by Zener [17]:

$$A = \frac{2C_{44}}{C_{11} - C_{12}} \quad (I.13)$$

For isotropic crystals A=1, on the other hand if A≠1 the materials are anisotropic [18].

I. 8. 3. Anisotropy factor

The relative variation in volume V under the effect of an applied hydrostatic pressure defines the compressibility modulus of a material (in English Bulkmodulus) denoted B. Its expression as a function of elastic constants is as follows [19]:

$$B = \frac{1}{3}(C_{11} + 2C_{12}) \quad (I.14)$$

I. 8. 4. Shear modulus

The shear or rigidity modulus is a physical quantity specific to each material and which is involved in the characterization of deformations, under a certain angle, caused by shear forces.

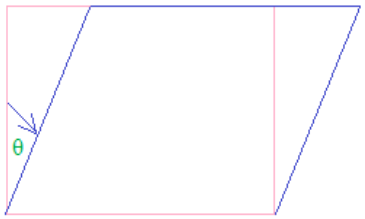

Fig. I. 9. A shear test.

Hill's shear modulus G is expressed by the following relation:

$$G = \frac{\sigma}{\theta} = \frac{g_V + g_R}{2} = \frac{C_{11} - C_{12}}{2} \qquad (I.15)$$

Where g_V and g_R are respectively the Voigt shear modulus and the Reuss shear modulus for cubic structures [18,19] expressed by:

$$g_V = \frac{C_{11}-C_{12}+3C_{44}}{5} \text{ , } g_R = \frac{5C_{44}(C_{11}-C_{12})}{4C_{44}+3(C_{11}-C_{12})} \qquad (I.16)$$

I. 8. 5. Young's modulus

Young's modulus, also called (longitudinal) elasticity modulus or tensile modulus, is the constant linking the tensile stress **σ** to the deformation **ε** of a material as long as it is elastic and isotropic. It can be expressed as a function of elastic constants or as a function of Lamé coefficients or as a function of Hill's compressibility B and shear moduli G, by the following formulas [20]:

$$E = \frac{\mu(3\lambda + 2\mu)}{(\lambda + \mu)} = \frac{C_{12}(3C_{12} + 2C_{44})}{(C_{12} + C_{44})} = \frac{9BG}{3B + G} \qquad (I.17)$$

I. 8. 6. Poisson coefficient

Poisson's ratio υ represents the contraction of the material perpendicular to the direction of the applied force or its elongation [18].

Its expression is given by:

$$\upsilon = \frac{(l_0-l)/l_0}{(L-L_0)/L_0} = -\frac{\Delta l/l_0}{\Delta L/L_0} \qquad (I.18)$$

Figure I.6 shows the longitudinal and transverse deformations that a specimen undergoes under applied stress:

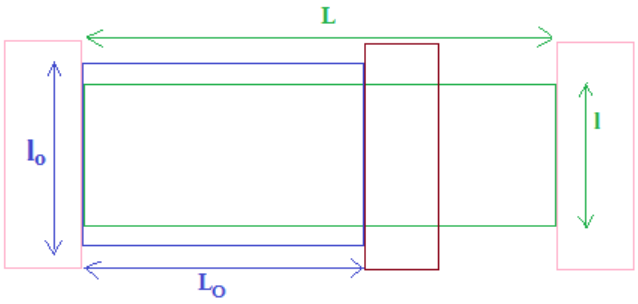

Fig. I. 10. Orientation of different deformations of a specimen.

For small deformations, the change in volume ΔV/V due to the deformation of the material is

$$\frac{\Delta V}{V_0} = (1 - 2\upsilon)\frac{\Delta L}{L_0} \qquad (I.19)$$

We can also express the Poisson's ratio from the elastic constants or as a function of the Lamé coefficients or also as a function of the compressibility modulus B and that of Hill's shear G:

$$\upsilon = \frac{C_{12}}{2(C_{12} + C_{44})} = \frac{\lambda}{2(\lambda + \mu)} = \frac{3B - 2G}{2(3B + G)} \qquad (I.20)$$

It is important to note that Poisson's ratio reflects the nature of the bonds in the substance.

I. 9. Electronic properties

I. 9. 1. Energy Bands

The electrons in an isolated atom have well-defined permitted energy levels, however if they are in a lattice of a crystal their behavior will be different [21]. Indeed, in elements with a short interatomic distance, the presence of neighboring atoms generates interference between the permitted levels of each atom, leading to very close and quasi-continuous states nicknamed energy bands (**Fig. I. 12.**).

Materials are characterized by their electrons located in energy bands separated by forbidden bands or energy holes or even gaps. The completely filled valence band is what is called the highest permitted occupied band, unlike the conduction band which is the lowest permitted empty band.

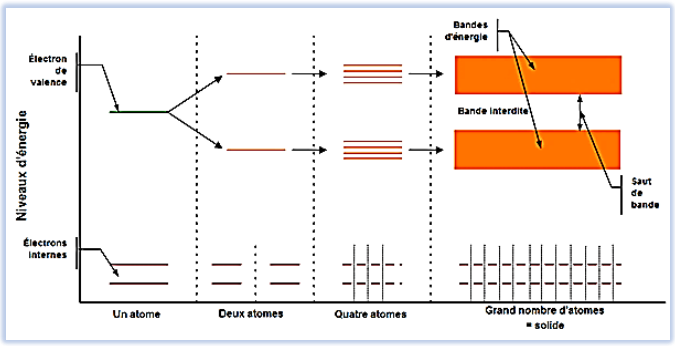

Fig. I. 11. Broadening of energy levels as the number of atoms gathered increases.

I. 9. 2. Electronic structure

The band structure of a semiconductor is very important for studying optical transitions and photoemissions as well as the creation of optoelectronic devices. It makes it possible to determine the nature of the gap and its value, as well as the possible optical transitions. We represent the energy diagram by studying the energy as a function of the wave vector, in a crystallographic direction of the reciprocal network. This diagram shows the ends of the conduction and valence bands as well as the different points of high symmetry, in the first Brillouin zone of the reciprocal space (**Fig. I. 12.**).

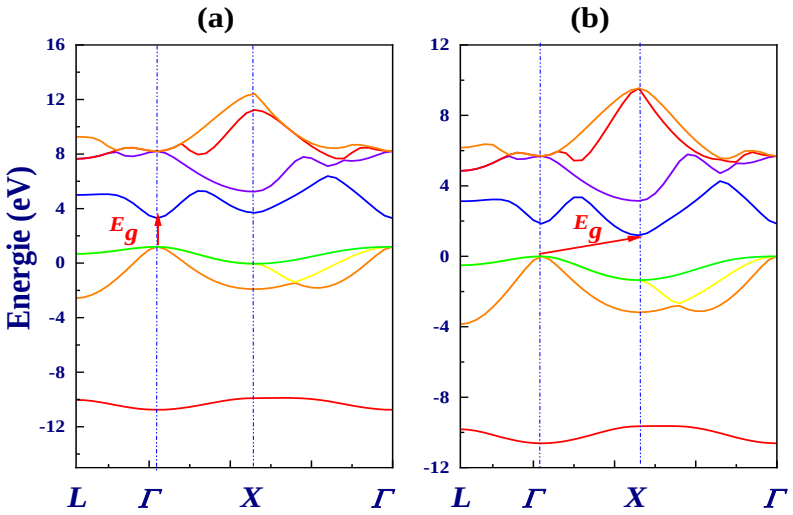

Fig. I. 12. Diagram of a band structure
(valence band in green and conduction band in blue).

I. 9. 3. Gap direct

We say that the gap is direct when the maximum of the valence band and the minimum of the conduction band are located at a value close to the wave vector k on the energy diagram at the center of the Brillouin zone **(fig.I.12 (a)).** The minimum energy transition between these two bands can take place without a change in wave vector, allowing the absorption and emission of light much more efficiently. In light emission applications, direct gap materials are preferred. Indeed, as the band ends are located at similar values of k, the probability of radiative recombination of the carriers is high.

I. 9. 4. Gap indirect

The gap is said to be indirect when the maximum of the valence band and the minimum of the conduction band are located at distinct values of the wave vector k, in the Brillouin zone **(fig.I.12 (b)).** The electronic transition between the top of the valence band and the bottom of

the conduction band, occurring with a change in wave vector, is accompanied by the change in the momentum of the electrons ($\Delta p \vec{} = \hbar \Delta k \vec{} \neq 0 \vec{}$) and their conduction band corresponds to electrons of high effective mass, which causes their low mobility.

I. 9. 5. Electron density of states

The total electron density makes it possible to know the electronic distribution and the number of electronic states of given energy, specifies the nature of bonds between the elements constituting the material and shows the origin of its electronic and optical properties.

The treatment of this density is done in direct space, because it is obtained by integration, over the Brillouin zone, using the tetrahedron method [18]. The projection of the total electron density, onto the orbitals s, p, d and f, gives the partial electron density which provides information on the physical and chemical properties of the materials.

I. 10. Optical properties for non-metallic materials

Non-metallic materials consist of various energy band structures. Thus, all four optical phenomena such as absorption, reflection, transmission and refraction are important for these materials.

I. 10. a Refraction

when light photons are transmitted through a material, they causes polarization of the electrons and in-turn the speed of light is reduced and the beam of light changes direction.

The relative velocity of light passing through a medium is expressed by the optical property called the index of refraction (n), and is defined as

$$n = \frac{C_0}{C} \qquad (I.21)$$

where c_0 *is the* speed of light in vacuum and c *the* speed of light in the concerned material.

Fig. I. 13**.** Show the incidence beam , reflected beam and refracted beam in solid material , if the angle of incidence from a normal to the surface is θi, and the angle of refraction is θr, the refractive index of the medium, n, is given by (provided that the incident light is coming from a phase of low refractive index such as vacuum or air)

$$n = \frac{\sin(\theta_i)}{\sin(\theta_r)} \qquad (I.22)$$

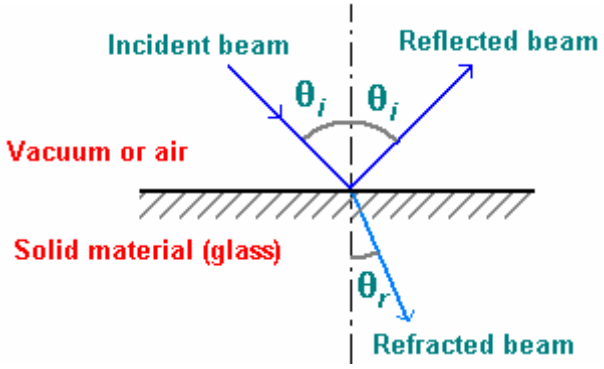

Fig. I. 13. Diagram of of incidence beam , reflected beam and refracted beam in solid material

The speed of light in a material can be related to its electrical and magnetic properties as

$$c = \frac{1}{\sqrt{\mu \times \varepsilon}} \tag{I. 23}$$

where ε – electrical permittivity, and μ – magnetic permeability. Thus,

$$\boldsymbol{n = \frac{C_0}{C} = \frac{\sqrt{\mu \times \varepsilon}}{\sqrt{\mu_0 \times \varepsilon_0}} = \sqrt{\mu_r \times \varepsilon_r}} \tag{I. 24}$$

Since most materials are only slightly magnetic i.e. $\mu r \approx 1$, Thus

$$\boldsymbol{n = \sqrt{\varepsilon_r}} \tag{I. 25}$$

Thus, for transparent materials, index of refraction and dielectric constant are related, **Table I.1** show values of refractive indices for some materials:

Table I.1 the refractive index values for various semiconductors materials.

Material	Refractive index	Material	Refractive index
Air		Epoxy	
Ice	1.309	Polystyrene	1.6
Water	1.33	Spinel, $MgAl_2O_3$	1.72
Teflon	1.35	Sapphire, Al_2O_3	1.7
Silica glass	1.458	Rutile, TiO_2	2.8
Polymethyl methacrylate	1.49	Diamond	2.17
Silicate glass	1.5	Silicon	3.29

CHAPTER II

AB-INITIO METHODS AND SIMULATION TOOL

II .1. Introduction

Ab-initio quantum simulations make it possible to explore the structural and electronic properties of matter, without a priori experimental knowledge of the systems studied. They use atomic constants as input parameters in the resolution of the Schrödinger equation without using adjustable variables and rely on density functional theory (DFT), the development of which was highlighted by Hohenberg, Kohn and Sham [22, 23].

These methods, from solid-state physics which corresponds to DFT treating electron density rather than the wave function and which earned Walter Kohn the Nobel Prize in Chemistry in 1998, make it possible to treat a few tens to a few hundred atoms while remaining within the limits of the precision of Hartree-Fock type methods [24]

II .2. Schrödinger equation

The description of the physical and chemical properties of a crystal system consists of solving the stationary and non-relativistic Schrödinger equation describing this problem:

$$H\Psi = E\Psi \quad \text{(II. 1)}$$

Or

- Ψ : is the wave function which contains all the information of the system studied.
- E : is the self-energy of the system (ground state).
- H : is the total Hamiltonian of the system formed by N_e electrons and N_n nuclei [25, 26]

$$H = T_e + T_n + V_{e-e} + V_{n-n} + V_{e-n} \quad \text{(II. 2)}$$

With

$$T_e = -\frac{\hbar^2}{2}\sum_{i=1}^{N_e}\frac{\Delta_{r_i}}{m_e} \quad \text{(II. 3)}$$

is the kinetic energy of the electrons, even the mass of each of them.

$$T_n = -\frac{\hbar^2}{2}\sum_{i=1}^{N_n}\frac{\Delta_{R_i}}{M_n} \quad \text{(II. 4)}$$

is the kinetic energy of the nuclei, M_n is the mass of each of them.

$$V_{e-e} = \frac{1}{8\pi\varepsilon_0}\sum_{i\neq j}\frac{e^2}{|\vec{r}_i-\vec{r}_j|} \quad \text{(II. 5)}$$

is the potential energy of repulsive electron-electron interaction.

$$V_{n-n} = \frac{1}{8\pi\varepsilon_0}\sum_{i\neq j}\frac{Z_i Z_j e^2}{|\vec{R}_i-\vec{R}_j|} \quad \text{(II. 6)}$$

is the potential energy of repulsive core-nucleus interaction.

$$V_{e-n} = \frac{-1}{4\pi\varepsilon_0}\sum_{i,j}\frac{Z_i e^2}{|\vec{R}_i - \vec{r}_j|} \quad \text{(II. 7)}$$

is the potential energy of attractive electron-nucleus interaction.

$$\vec{r}_{i,j}(i,j = 1,2,\dots,N_e) \quad \text{(II. 8)}$$

are the position vectors of the electrons, N_e is the number of electrons.

$$\vec{R}_{i,j}(i,j = 1,2,\dots,N_n) \quad \text{(II. 9)}$$

are the position vectors of the nuclei, N_n is the number of nuclei.

$\hbar = \frac{h}{2\pi} = 1{,}05\ 1034$ J.s : is Planck's constant.

ε_0 : is the vacuum permittivity, with $4\pi\ \varepsilon_0 = 1{,}11256.10^{-10}J^{-1}C^2m^{-1}$

e : is the charge of the electron.

The solution to such a problem as well as its possible analytical representation promises to be a difficult task given the limited memory of computer tools. However, it is possible to reformulate the problem by employing suitable theorems and approximations such as the Born Oppenheimer approximation, the Hartree-Fock approximation...

II .3. Born-Oppenheimer approximation (adiabatic)

This approximation is the first of the approximations used for solving the Schrödinger equation. Because nuclei are heavier than electrons (M_n≫m_e), this allows them to move very slowly compared to electrons (quasi-static). They therefore appear to be immobile relative to the electrons.

Born and Oppenheimer then neglected the movement of the nuclei in relation to that of the electrons which adapt instantly to the slowly variable configuration of the nuclei, hence the adiabatic notion [27].

This approximation also neglects the kinetic energy T_n of the nuclei and the nucleus-nucleus interaction potential energy V_(n-n) which is practically constant [28], which reduces the electronic Hamiltonian:

$$H_e = T_e + V_{n-e} + V_{e-e} \quad \text{(II. 10)}$$

Thus, the Schrödinger equation takes the following form:

$$H_e\Psi = E_e\Psi \quad \text{(II. 11)}$$

Because of the electron-electron interaction, the resolution of the Schrödinger equation remains complex for many bodies, so other additional approximations are resorted to.

II.4. Hartree approximation

In 1928, Douglas Hartree proposed this approximation [29, 30] which is based on the free electron hypothesis and does not take into consideration the electron-spin interaction. Each of them moves in the mean field created by the other electrons and by the nuclei and can then be described by its own wave function.

The Schrödinger equation with several interacting electrons is reduced to several Schrödinger equations (with an independent electron) called Hartree equations [31] which are written in the form:

$$\left[-\frac{\hbar^2}{2m_e}\Delta + V_{ext}(\vec{r}) + V_H(\vec{r})\right]\Psi_i(\vec{r}_i) = E\Psi_i(\vec{r}_i) \qquad \text{(II. 12)}$$

Or $V_{ext}(\vec{r})$ explains the Coulomb attractive interaction between the electron and the nuclei and $V_H(\vec{r})$ represents the potential of Hartree.

The global wave function is thus the product of elementary wave functions describing the state of a particular electron [32]:

$$\Psi(\vec{r}) = \prod_{i=1}^{N_e}\Psi_i(\vec{r}_i) \qquad \text{(II. 13)}$$

The anti-symmetrization of the electronic wave function, by permuting two electrons for example, is written:

$$\Psi_e(\vec{r}_1, \vec{r}_2, \dots, \vec{r}_{N_e}) = -\Psi_e(\vec{r}_2, \vec{r}_1, \dots, \vec{r}_{N_e}) \qquad \text{(II. 14)}$$

Such a description therefore obeys the Pauli exclusion principle which requires that two electrons with the same quantum numbers cannot simultaneously occupy the same quantum state. However, in Hartree's formulation of the wave function, this is not the case, because electron i occupies precisely state i. Not being antisymmetric with respect to the exchange of any two electrons, the solutions of the Hartree equation violate the Pauli exclusion principle.

In conclusion, this approximation will not be able to transform the N-body equation into a set of independent equations.

II.5. Hartree-Fock approximation

Taking into account the effect of electron spin (Pauli exclusion principle), Fock wrote the wave function in the form of a Slater determinant:

$$\Psi_e(q_1, q_2, \dots, q_{N_e}) = \frac{1}{\sqrt{N_e!}} \begin{vmatrix} \Psi_1(q_1) & \dots & \Psi_1(q_{N_e}) \\ \vdots & \ddots & \vdots \\ \Psi_{N_e}(q_1) & \cdots & \Psi_{N_e}(q_{N_e}) \end{vmatrix} \quad \text{(II. 15)}$$

Or

- N_e : is the number of electrons.
- q_i : represents a combination of four variables (the three variables of the space (x_i, y_i, z_i) and the fourth variable S_z representing the projection of the spin of electron i on the z axis).
- $\Psi_i(q_i)$: are the mono-electron wave functions, with $(i = 1,2, \dots, N_e)$.

In this approximation the single-electron Hamiltonian contains a term which describes the classical Coulomb interaction between electrons (Hartree term) and an additional purely quantum term (exchange term) which results from the application of the Pauli principle.

The Hartree-Fock approximation therefore makes it possible to approach the N-body problem as a one-body problem, in which each electron is subject to an effective potential which is, in part, generated by the other electrons. To solve the one-electron Hamiltonian, we proceed as follows [33]:

- ✓ We assume a spatial distribution of nuclei, which determines the interaction energy between nuclei as well as the Hartree potential at any point in space.
- ✓ To coherently solve single-electronic equations $H_e\Psi_e = E_e\Psi_e$, we choose an initial base of orbitals, generally atomic orbitals or plane waves.
- ✓ Using this base, we calculate the interaction potentials which we introduce into the mono-electronic equations.
- ✓ This resolution is then possible and provides a second set of mono-electronic functions from which we re-evaluate the interaction potentials, and we repeat the procedure until we obtain a set of mono-electronic wave functions. electronics as well as the eigenvalues which no longer evolve (stationary values).
- ✓ Then, we calculate the total energy of the system of atoms and we adjust the spatial distribution of the nuclei so as to minimize this total energy.

The calculation of the Slater determinant is very cumbersome from a numerical point of view, hence the introduction of the density functional method which considerably simplifies the calculations.

II.6. Density functional theory (DFT)

The basis of the density functional is that the energy of an electronic system can be expressed as a function of the ground state density $\rho(r)$.

Historically, the origin of DFT (Density Functional Theory) returns to the theoretical model developed in 1920 by Thomas and Fermi [34, 35] followed in the 1960s by the contributions of Hohenberg and Kohn on the one hand [22] and Kohn and Sham on the other hand [23]. The Thomas-Fermi model is interesting in the sense that it constitutes the first step towards a theory where the complicated calculation of the wave function dependent on 3N spatial coordinates is replaced by that of a simpler function which is the electron density dependent only on 3 spatial coordinates and is given by [36]:

$$\begin{cases} \int\int \rho(r)dr = N_e \\ \rho(r \to \infty) = 0 \end{cases} \qquad \text{(II. 16)}$$

It is in this spirit that in 1964, Hohenberg and Kohn formulated and demonstrated two theorems where they put the previous ideas into a mathematical framework [22]. These two theorems are the pillars of DFT as it is accepted today.

II. 6. 1. Hohenberg-Kohn theorems

The two Hohenberg-Kohn theorems apply to any system of N_e interacting electrons, in an external potential V_{ext} [22]:

II.6.1.1. First theorem

Any physical property of a system N_e electrons subjected to the effect of a static external potential V_{ext} s'written, in its ground state, as a functional of the electron density $\rho(r)$. Therefore, the total energy of the system in the ground state is also a functional only of the electron density $E = E[\rho(r)]$.

II.6.1.2. Second theorem

There is a universal functionality $E(\rho)$ which expresses the energy as a function of the electron density $\rho(r)$, valid for any external potential V_{ext}. For a potential V_{ext} et a number of electrons N_e, the energy of the ground state of the system is the value which minimizes this functional and the density $\rho(r)$ associated with it corresponds to the exact density $\rho_0(r)$ of the ground state [37] :

$$\left.\frac{dE[\rho(r)]}{d\rho(r)}\right|_{\rho=\rho_0} = 0 \Rightarrow E(\rho_0) = \min E(\rho) \quad \text{(II. 17)}$$

The functional of the total energy of the ground state is written as follows:

$$E[\rho(r)] = F_{HK}[\rho(r)] + \int V_{ext}(r)\,\rho(r)\,dr \quad \text{(II. 18)}$$

Or $F_{HK}[\rho(r)]$ is the universal functional of a system with many electrons:

$$F_{HK}[\rho(r)] = T_e[\rho(r)] + V_{e-e}[\rho(r)] \quad \text{(II. 19)}$$

$T_e[\rho(r)]$et$V_{e-e}[\rho(r)]$ are respectively the functionals of the density relative to the kinetic energy of the electron and to the electron-electron interaction.

The second theorem of Hohenberg and Kohn presents a disadvantage for its direct application in practice, because the form of the functional $F_{HK}[\rho(r)]$ is unknown. So it is relatively difficult to determine the ground state energy in an external potential. This problem can be circumvented by the Kohn and Sham approximation. [23].

II. 6. 2. Kohn and Sham approximation

To determine the exact properties of a multiparticle system, Kohn and Sham proposed an approach that uses independent particle methods. The functional energy is given by [23, 38] :

$$E_{KS}[\rho(r)] = T_e[\rho(r)] + E_H[\rho(r)] + E_{xc}[\rho(r)] + \int \rho(r)\,V_{ext}(r)\,d^3r \quad \text{(II. 20)}$$

$E_{KS}[\rho(r)]$ is an exchange-correlation functional,$T_e[\rho(r)]$ is the kinetic energy of the system $N_e$éelectrons without interaction in an effective potential, and $E_H[\rho(r)]$ is the Hartree energy or the Coulomb interaction energy and $V_{ext}(r)$e st the external potential created by the nuclei.

$$E_{KS}[\rho(r)] = F[\rho(r)] + \int \rho(r)\,V_{ext}(r)\,d^3r \quad \text{(II. 21)}$$

$F[\rho(r)]$ is the Kohn and Sham functional.

The ground state electron density of a system of interacting particles can be calculated as the ground state electron density of a noninteracting auxiliary system.

Thus, from the reformulation introduced by Kohn and Sham we define a mono-electron Hamiltonian and the resolution of the mono-electron Kohn-Sham equations is done

analytically. Its ground state wave function Ψ^{KS} is written exactly as a wave function given by a Slater determinant of single-electron orbitals $\Phi_i(r)$ which are called Kohn-Sham orbitals:

$$\left[-\frac{\hbar^2}{2m_e}\Delta + V_{eff}(r)\right]\Phi_i(r) = \varepsilon_i\Phi_i(r) \quad \text{(II. 22)}$$

ε_i is the energy corresponding to the Kohn-Sham orbital $\Phi_i(r)$ and i represents the level of the energy state of the system. The potential of KS is given by:

$$V_{eff}(r) = V_{ext}(r) + V_H(r) + V_{xc}(r) \quad \text{(II. 23)}$$

Or $V_H(r)$ expresses the classical Coulomb interaction between pairs of electrons (Hartree potential) and $V_{xc}(r)$ is the exchange-correlation potential defined as the derivative of $E_{xc}[\rho(r)]$depending on the electron density:

$$V_{xc}(r) = \frac{\delta E_{xc}[\rho(r)]}{\delta\rho(r)} \quad \text{(II. 24)}$$

With the density of the system being the expression given by:

$$\rho(r) = \sum_{i=1}^{N_e} |\Phi_i(r)|^2 \quad \text{(II. 25)}$$

So far DFT is an exact method, but for DFT and the Kohn-Sham equations to become usable in practice, we need to propose a formulation of $E_{xc}[\rho(r)]$ and for this it is necessary to approximate this energy. Two types of approximations exist, the local density approximation LDA and the generalized gradient approximation (GGA).

II. 6. 3. Local Density Approximation (LDA)

The local density approximation known as LDA (Local Density Approximation) makes it possible to transform DFT, a useless exact N-body theory, into an approximate but very useful (and widely used) theory. The electron density is treated locally, in this approximation, in the form of a uniform electron gas [39]. Each infinitesimal volume of the system contributes an exchange-correlation energy equal to that due to the contribution of a homogeneous gas. The latter occupies the same infinitesimal volume and has the same total charge density of the original material in that volume.

The exchange-correlation part of the total energy of the fundamental state of the system is written in the form:

$$E_{xc}^{LDA}[\rho(r)] = \int \rho(r)\,\varepsilon_{xc}[\rho(r)]\,dr \quad \text{(II. 26)}$$

$\varepsilon_{xc}[\rho(r)]$represents the exchange−correlation energy per electron in a system of mutually interacting electrons of uniform density ρ. It can be separated into an exchange term and a correlation term:

$$\varepsilon_{xc}^{LDA}[\rho(r)] = \varepsilon_{x}^{LDA}[\rho(r)] + \varepsilon_{c}^{LDA}[\rho(r)] \quad \text{(II. 27)}$$

The exchange-correlation potential is given by:

$$V_{xc}(r) = \varepsilon_{xc}^{LDA}[\rho(r)] + \rho(r)\frac{d\varepsilon_{xc}^{LDA}[\rho(r)]}{d\rho(r)} \quad \text{(II. 28)}$$

II. 6. 4. Generalized Gradient Approximation (GGA)

The Generalized Gradient Approximation (GGA [40]) is an improvement on LDA because it takes into account the inhomogeneity of the electron density. Indeed, the exchange and correlation energy is a function of the electron density and its gradient:

$$E_{xc}^{GGA}[\rho(r)] = \int \rho(r)\, \varepsilon_{xc}\left[\rho(r), \vec{\nabla}\rho(r)\right] dr \quad \text{(II. 29)}$$

Furthermore, there are different parameterizations of the GGA [41,42]. It should be noted, however, that the GGA approximation does not necessarily lead to better results than the LDA, it all depends on the property that we calculate and the system that we treat.

Generally speaking, they are particularly effective for improving the calculations of certain properties. Their major disadvantage is that such calculations are generally more demanding in computer resources than for classical functionals, due to the incorporation of Hartree-Fock terms.

II. 6. 5. Cycle auto-cohérent [21]

To determine the eigenstates and eigenfunctions, we solve the Kohn and Sham equation by a self-consistent calculation. This resolution is done in an iterative manner using a self-consistent cycle of iterations. The different stages of the self-consistent cycle of DFT are as follows (Figure II.1.):

1- Start with a test density for the first iteration.
2- Calculate the density and exchange potential correlation for a point.
3- Construct the Hamiltonian.
4- Solve the Kohn-Sham equation.
5- Calculate the new electron density.
6- Check the convergence criterion (by comparing the old and new density).
7- Calculate the different physical quantities (Energy, forces, etc.), End of calculation.

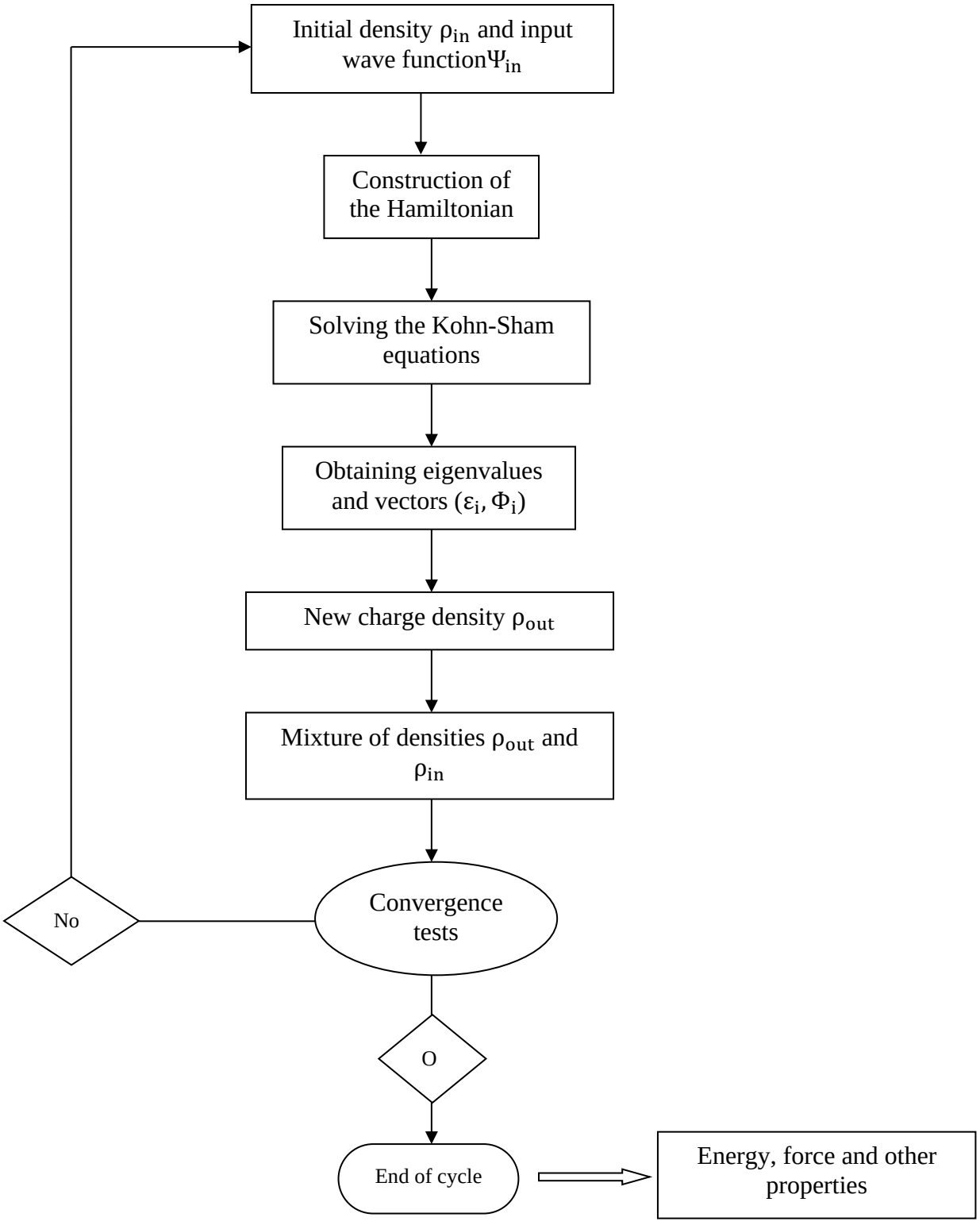

Figure II.1. Representation of the self-consistent cycle in the resolution Kohn-Sham equations [43].

II.7. Pseudo-potential method

II.7.1. Introduction

The physical properties of solids depend on the valence electrons more than those of the core and the investigation of some of these properties, namely the electronic properties, is more precise with the pseudo-potential method [44-45]. In fact, we approximate the configuration of these core electrons in the solid to that of an isolated atom. This consideration makes it possible to group them with the nucleus, to constitute rigid ions which we call the frozen core approximation [46]. In this approximation, the Coulomb interaction potential of the nucleus and the effects of the core electrons is replaced by an effective potential that interacts with the valence electrons only [47].

II.7.2. Bloch's theorem

This theorem shows that the solutions of the Schrödinger equation, for a periodic potential, can be put in a new form of a product of a plane wave by a function $u_i(\vec{r})$ which has the periodicity of the crystal lattice [28] :

$$\Psi_i(\vec{r}) = u_i(\vec{r}) \exp(i\vec{k}\vec{r}) \qquad (II.30)$$

with: $u_i(\vec{r}) = u_i(\vec{r} + \vec{R})$,$\vec{k}$ is the wave vector, i is the band index, $\vec{R}$ is the vector of the direct network.

Function $u_i(\vec{r})$ can be written as a sum:

$$u_i(\vec{r}) = \sum_G C_{iG} \exp(i\vec{G}\vec{r})) \qquad (II.31)$$

Or $\vec{G}$ is a vector of the reciprocal network defined by $\vec{G}.\vec{R} = 2\pi m$ (m is an integer).

Replacing $u_i(\vec{r})$ in (23) by his expression (24), we will have:

$$\Psi_{ik}(\vec{r}) = \sum_G C_{i,\vec{k}+\vec{G}} \exp(i(\vec{k} + \vec{G})\vec{r}) \qquad (II.32)$$

The infinity of electrons in a solid is taken into account by an infinity of k points and at each k point only a limited number of electronic states are occupied. The boundary conditions determine a precise set of points k.

Because of the infinite number of points k and their occupied states, an infinite number of calculations are necessary to obtain the density n(r), the electronic potential V(r) and the total energy E.

Electronic wave functions can be presented by a wave function at a single point k, in a region of space k, because of the identity of these functions at their identical k points. Which requires us to determine electronic states at a finite number of points k for the calculation of potential and energy.

The calculation of electronic states, proposed by several methods, at a small number of special points k, in the Brillouin zone, made it possible to have good approximations of the electronic potential and the total energy.

II.7.3. Sampling of the first Brillouin zone

The problem of solving the Schrödinger equation of an infinite number of wave vectors k of the reciprocal lattice, in a crystal, occupying this space in a discrete but quasi-continuous manner, requires the sampling of the first zone of Brillouin to properly calculate the electronic structure of a finite and minimal number of points k, where the electronic states are occupied and characterized by continuous bands. The Monkhorst and Pack method [48] is one of the sampling methods that have been proposed to calculate the electronic potential in the first Brillouin zone.

II.7.4. Breaking energy

The need for a very large number of plane waves to represent the wave function led, in 1992, M.C. Payne et al [49] to prove that the coefficients C_{k+G} dplane waves having low kinetic energy $\frac{\hbar^2}{2m}|k+G|^2$ are larger than those associated with plane waves with large kinetic energy. Thus, the maximum limit of this energy is called the cut-off energy verifying:

$$\frac{\hbar^2}{2m}|k+G|^2 \leq E_{cut-off} \qquad \text{(II. 33)}$$

$$E_{cut-off} = \frac{\hbar^2}{2m}|k+G_{max}|^2 \qquad \text{(II. 34)}$$

The selection of plane waves consists of a sphere of radius G_{max} centered at the origin of the reciprocal space by imposing the condition $|k+G| \leq G_{max}$. Cette sphère contient un certain nombre d'ondes planes, donné par l'expression :

$$N_{PW} \approx N_k \cdot \frac{1}{2\Pi^2} V_s E_{cut-off}^{\frac{3}{2}} \qquad \text{(II. 35)}$$

Or $N_k$et V_s are respectively the number of vectors $\vec{k}$ sampled in the first Brillouin zone and the volume of the simulation cell. Limitation of the plane wave basis induces errors in the

calculation of the total energy [50]. A certain degree of accuracy of the calculation is well determined, following the appropriate choice of the cut-off energy which leads to a convergence of the total energy.

II.7.5. Frozen Heart Approximation

"Freezing the core electrons and only treating the valence electrons" constitutes the frozen core approximation and is overall the basic idea of the pseudo-potential method. In this model and in the Kohn and Sham equations, the real effective potential is replaced by a lower potential, felt by the valence electrons, following the screening of the nucleus by the core electrons. Thus, the wave functions of the valence electrons become pseudo-wave functions [51-52].

II.7.6. Construction of the pseudo-potential

Among the various known pseudo-potentials, we will limit ourselves to the pseudo-potential with conserved norm and the ultra-soft one:

II.7.6.a. Pseudo-potential with conserved norm

In this type of pseudo-potential, the conservation of the norm is present (the charge contained in the core region converges towards the real charge in this region). Based on ab-initio atomic calculations, extractions of the pseudo-potential with conserved norm were proposed in 1979 by Hamann et al. [53], then in 1982 by Bachelet et al. [54] and again Hamann in 1989 [55]. They were thus able to tabulate the pseudo-potentials of all the elements of the periodic table.

This pseudo-potential consists of the resolution of the Schrödinger equation for an isolated atom having a wave function dependent on the three quantum numbers (n, l, m) :

$$\varphi_{n,l,m}(r,\Theta,\xi) = R_{n,l}(r).Y_{l,m}(\Theta,\xi) \qquad \text{(II. 36)}$$

Or $R_{n,l}$ et $Y_{l,m}$ are respectively the radial part and the spherical harmonics of the wave function. A unique consideration of the radial part of the wave function $R_{n,l}$ was imposed from the spherical symmetry of the atom.

In the concept of pseudo-potentials with conserved norm, the following conditions are satisfied [50]:

- ✓ The eigenvalues of the pseudo-radial and real wave functions are equal.

- ✓ Real wave functions and pseudo wave functions are equal beyond the cutoff radius.
- ✓ Inside the cutoff radius, the pseudo-wave function and the valence wave function are different but their norms are the same.La pseudo-fonction d'onde ne possède pas de nœuds.
- ✓ The pseudo potential varies continuously (the first and second derivatives of the pseudo-wave function and the real wave function are equal for r = cut-off radius).
- ✓ The orbitals associated with the core and valence electrons do not overlap.
- ✓ The norm is preserved (the charge density in the core region is the same for the pseudo-wave functions and the real wave functions for each valence state).

II.7.6.b. Pseudo-potentiel ultra soft 'doux' (US-PP)

In this pseudo-potential category, the charge contained in the core region is different from the actual charge in that region. It is in the case of materials carrying localized valence orbitals, such as rare earths or transition metals, that Vanderbilt [56] presents this ultra-soft pseudo-potential, which replaces that with a conserved norm, because the name d Ultra soft is the result of arbitrary smoothing of pseudo-wave functions in the heart region. This type of pseudo-potential restricts the number of plane waves (reduction of the cut-off energy) and uses a cut-off radius larger than that of pseudo-potentials with a conserved norm.

II.7.6.c. Application of the pseudo-potential

These pseudo-potentials are applicable according to two possibilities:

- ✓ Ab-initio (theoretical) approaches which are used to predict certain previously unknown physical properties, based on fundamental principles to solve the problems.
- ✓ The empirical method which adjusts certain parameters using experimental data (energy gaps).

II.7.6.d. Generation of the pseudo-potential

This consists of carrying out an atomic calculation for a configuration taken as a reference. Also, the appropriate choice of an element (atomic number, electronic configuration) and an exchange and correlation functional allows, by choosing the orbitals like those of

valence, the determination of the proper energies and the proper states of the isolated atom. We cite two methods for generating the pseudo-potential [57]:

1- We conceive the pseudo-potential from the inversion of the Schrödinger equation with the pseudo-wave functions and the subtraction of the contributions of the Hartree energy and the exchange-correlation energy, for the electrons of valence. Thus, we generate the pseudo-potential from the pseudo-valence wave functions taken so that they coincide with the wave functions of the valence electrons, outside the cut-off radius and respecting the conditions imposed, in the region of the heart.
2- A choice of a parameterized pseudo-potential is important once the eigenenergies and valence eigenstates of the isolated atom are determined. Subsequently, we improve the cut-off radius so that the calculation on the pseudo-atom gives us clean energies equal to those found previously in the old step and pseudo-valence functions equal to the wave functions of the electrons, beyond the choice of the cut-off radius taken.

II.7.7 The linearized augmented plane wave method or FP-LAPW

The linearized augmented plane wave method differs from that of the pseudopotential previously described, it is quite general and well suited to many problems. The so-called augmented plane wave or APW method was introduced by Slater [58, 59], then taken up by Andersen [60], it was improved and transformed into a new linear method called the LAPW method.

The FP-LAPW method belongs to the so-called all-electron methods which take into account the fact that electrons interact strongly and we cannot therefore omit the effect of any of them. We must then look for a method that allows us to solve the Kohn-Sham equations while keeping the total potential and treating all the electrons.The APW method being the 'direct parent' of the FP-LAPW, we consider it necessary and natural to fully understand what it consists of.

II.7.8. The APW method

In 1937, Slater [58] developed the APW method by noticing that in the vicinity of an atomic nucleus, the potential and the wave functions should be of the "Muffin-Tin" (MT) type, the latter i.e.d. the potential and wave functions are similar to those of an atom; they vary strongly but have spherical symmetry inside any MT sphere of radius.

Furthermore, in the space between atoms, the potential and wave functions can be considered smooth. From the above, the wave functions of the electrons in the crystal are then developed in different bases depending on the region considered: Radial solutions of the Schrödinger equation inside the MT sphere and plane waves in the interstitial region (Figure (II.2).

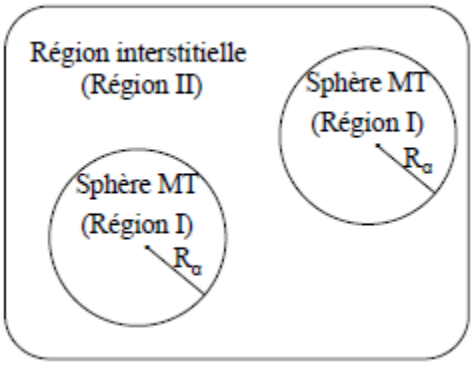

Figure II.2: Distribution of atomic unit cells in muffin tin spheres (S) radius and an interstitial region (I) adopted in the APW method.

The wave function is then of the form:

$$\phi(r) = \begin{cases} \frac{1}{\Omega^{\frac{1}{2}}} \sum_G C_G e^{i(G+K)r} & r \in I \\ \sum_{lm} A_{lm} U_l(r) Y_{lm}(r) & r \in S \end{cases} \qquad \text{(II-37)}$$

Above represents the radius of the sphere M_T, Ω the volume of the elementary cell while and are the coefficients of the development in spherical harmonics. The function is a regular solution of the Schrödinger equation for the radial part which in Rydberg units is written in the form:

$$\left\{ -\frac{d^2}{dr^2} + \frac{l(l+1)}{r^2} + V(r) - E_l \right\} r U_l(r) = 0 \qquad \text{(II-38)}$$

Where E_i: energy parameter.

$V(r)$: The spherical component of the potential in the sphere.

The radial functions defined by the previous equation are orthogonal to any eigenstate of the heart, but this orthogonality disappears on the limit of the sphere [58]. As shown in the following equation:

$$(E_1 - E_2) rU_1U_2 = U_2 \frac{d^2 rU_1}{dr^2} - U_1 \frac{d^2 rU_2}{dr^2} \quad \text{(II-39)}$$

U_1, U_2: are the radial solutions for these energies and respectively.

Slater made a particular choice for the wave functions, he shows that plane waves are the solutions of the Schrödinger equation in a constant potential. Whereas, radial functions are the solution in the case of spherical potential. So, it proves that E_l is equal to the eigenvalue E. This approximation is very good for materials with a face-centered cubic structure, and becomes less and less satisfactory with the reduction in symmetry of the material [58].

To ensure the continuity of the function on the surface of the MT sphere, the Alm coefficients must be developed according to the CG coefficients of the existing plane waves in the interstitial regions. Thus, after some algebraic calculations [61], we find that:

$$A_{lm} = \frac{4\pi i^l}{\Omega^{1/2} U_l(R_{MT})} \sum C_G J_l(|K+g| R_{MT}) Y_{lm}^*(K+G) \quad \text{(II-40)}$$

J_i: The Bessel function.

Where the origin is taken at the center of the sphere and is its radius, Thus the A_{lm} are completely determined by the plane wave coefficients, and the energy parameters E_l are variational coefficients in the method (APW).

The wave functions behave like plane waves in the interstitial region, and they increase in the core region and behave like radial functions. For the energy El, the APWs functions are solutions of the Schrödinger equation, with El equals the energy band indexed by G. This meant that the energy bands cannot be obtained by simple diagonalization, and this involves treating the secular determinant as a function of energy. Among the problems encountered in the APW method we cite:

The lack of variational freedom due to the fixation of which leads to the fact that the energies in the different energy bands for a given point k cannot be obtained by a single diagonalization. It is then necessary to treat the secular determinant as a function of energy.

In equation (II-40) the relation of the coefficient, A_{lm},$U_l(R_{MT})$ appears in the denominator, and it can happen that for values of the energy parameter, A_{lm},$U_l(R_{MT})$ vanishes at the limit of the sphere, and hence, this leads to the separation between radial functions and plane waves. The coefficients diverge. This will lead to numerical difficulties, this is called the asymptote problem.

To overcome these difficulties, several modifications have been made to the APW method, notably those proposed by Koelling [62] and by Anderson [60].

In 1975, Anderson proposed a method in which the basis functions and their derivatives are continuous for a given energy. This choice resolves the problems encountered in the APW method, thus providing a flexible and precise band structure method. This method is called the linear augmented plane wave method LAPW.

The modification consists of representing the wave function ϕ(r) inside the sphere by a linear combination of the radial functions $U_l(r)$ and their derivatives $\dot{U}_l(r)$ with respect to the energy .

II.8. Simulation tool

There are a large number of calculation codes based on DFT, For example DMol3, VASP, GAUSSIAN, ABINIT, CRYSTAL, BigDFT.

In this work, we will use the ab-initio calculation code CASTEP (Cambridge Serial Total Energy Package Software) originally developed by Professor M. C. Payne [63, 64,65] and which is part of a set of digital simulation software called Material Studio (MS), marketed by Accelrys ©.

CASTEP allows to simulate properties, interfaces and surfaces for a wide range of material classes such as ceramics, semiconductors, metals... [66].

CHAPTER III

RESULTS AND DISCUSSION

III.1. Introduction

We provide a study on the inorgaic hexachlorometallate structure, which has the general stoichiometric formula A_2MB_6, with the cubic antifluorite structure of space group Fm3m. This series of double perovskites is attracting much attention from researchers because of their probable use as solar cells, photovoltaic absorbers, microwave semiconductor with a wide band gap and optoelectronic devices. We focus on double perovskites with the halide anion B = Cl and consider four compounds with varying M− site cations (Si, Ge, Sn, and Pb) and fixed the alcali metal A = Cs.

This type of double perovskites called molecular salts show an ionic character because of their assembly of cations and anions. Inorganic perovskites are materials where the conductivity is ensured by the transport of holes in solar cells based on mesoporous electrodes. The rapid evolution of inorganic perovskites materials is due to their use in solar cell and thermoelectric applications. M. Khuili et al. report a strong optical absorption in the ultraviolet region and adequate thermoelectric characteristics make Cs_2SnX_6 (X = Cl, Br, I) candidates for replacing expensive silicon cells in solar panels [67].

We present in this work a study on the morphology, electronic and optical characteristics of Cs_2MCl_6 (M = Si, Sn, Ge and Pb) double perovskites.

III.2. Calculations details

The WIEN2k code [68] as implemented in the augmented plane-wave functions plus local orbitals and GGA-mBJ approximation as exchange potential were used in the calculation process.

In the electronic characterisation, the modified Becke-Johnson exchange potential is utilized and employed to tackle the electron-electron correlation effect [69–70].

The first step in this type of calculation is to specify the important parameters that influence the time and precision of the calculation. The shelves of Muffin-tin (R_{MT}) are given in atomic units (a.u.). Values of $R_{MT}\ min$ that we used in calculation of Cs_2MCl_6 (M = Si , Sn, Ge and Pb) properties are based on two criteria:

1- Ensure the integration of the majority of core electrons into the sphere (Muffin-tin).

2- Avoid overlapping spheres (Muffin-tin).

- The cutoff parameter R$Kmax$ = R_{MT} $min.Kmax$, with R_{MT} min is the smallest radius of the sphere and $Kmax$ is the norm of the largest wave vector used for the development in plane waves of the eigenfunctions.
- The number of k-points is the smallest number to achieve convergence.

The R_{MT}.Kmax parameter, the muffin-tin radii (R_{MT}) of Cs, Si, Ge, Pb and k-points for the Brillouin zone integration are reported in Table III. 1.

Table III. 1. Values of $R_{MT}.K_{max}$, R_{MT} of each constituent and k-points of Cs_2MCl_6 (M = Si, Sn, Ge and Pb) double perovskites using GGA approximation.

	R_{MT}.Kmax	R_{MT} (Cs)	R_{MT} (B)	R_{MT} (Cl)	k-points
Cs_2SiCl_6	9	2.3	1.58	1.66	5000
Cs_2GeCl_6	9	2.5	2.32	2.10	5000
Cs_2SnCl_6	9	2.5	2.5	2.16	5000
Cs_2PbCl_6	9	2.5	2.5	2.19	5000

(k-points =10000) for optical properties

III.3. Structural properties

III.3.1 Crystal structure

The structure of Cs_2MCl_6 (M = Si, Sn, Ge and Pb) is such that "M" atoms are symmetrical fixed at 4a (0, 0, 0) positions, "Cl" atoms are at 24e (x, 0, 0) positions (where, x is the anion positional parameter), and "Cs" atoms are symmetrical fixed at 8e (l/4, l/4, l/4) positions. The structural configuration of Cs_2MCl_6 (M = Si, Sn, Ge and Pb) is presented in Fig. III. 1.

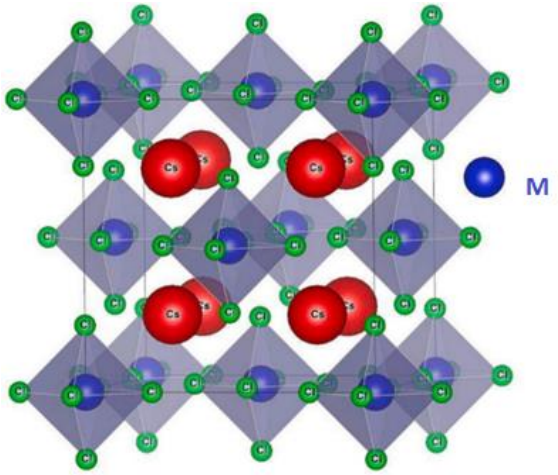

Fig. III. 1. The structural configuration of Cs_2MCl_6 (M = Si, Sn, Ge and Pb) double perovskites.

III.3.2 Determination of structural parameters of Cs_2MCl_6 (M = Si, Sn, Ge and Pb)

To determine the equilibrium lattice constant and to find how the energy total varies depending on this parameter, we carried out structural optimization on Cs_2MCl_6 (M = Si, Sn, Ge and Pb).

The calculation was explored with GGA approximation. Structural optimization is carried out by minimizing the total energy as a function of the volume V. The variation of energy as a function of volume for Cs_2MCl_6 (M = Si, Sn, Ge and Pb) is shown in Fig. III. 2.

The optimization cycle is repeated until convergence is reached. The equilibrium bulk modulus is evaluated by adjusting the curve of variation of the total energy as a function of volume obtained at the end of the cycle to the Murnaghan equation [71] given by:

$$E(V) = E_0 + \frac{B}{B'(B'+1)}\left[V\left(\frac{V_0}{V}\right)^{B'} - V_0\right] + \frac{B}{B'}(V - V_0) \quad \textbf{(III. 1)}$$

E_0: represents the ground state energy corresponding to volume V_0.

V_0: is the volume of the ground state.

The equilibrium lattice constant is given by the minimum of the curve $E_{tot}(V)$.

B: represents the bulk modulus determined by the following equation:

$$B = V\frac{\partial^2 E}{\partial V^2} \quad \textbf{(III. 2)}$$

B': is the derivative of the bulk modulus according to the pressue.

$$B' = V\frac{\partial B}{\partial P} \quad \textbf{(III. 3)}$$

We summarize in Table 2 the main structural properties of pure compounds. The lattice parameter for Cs_2SnCl_6 is closer the experimental value reported by Thomas B et al. [72] with a precision of 0.7%. The theoretical results of the lattice constant for the compound Cs_2SnCl_6 obtained by researcher Berri S [73] are very consistent with ours. Very satisfactory results in calculating the lattice constant of Cs_2PbCl_6 compound compared with the results published in the research [74].

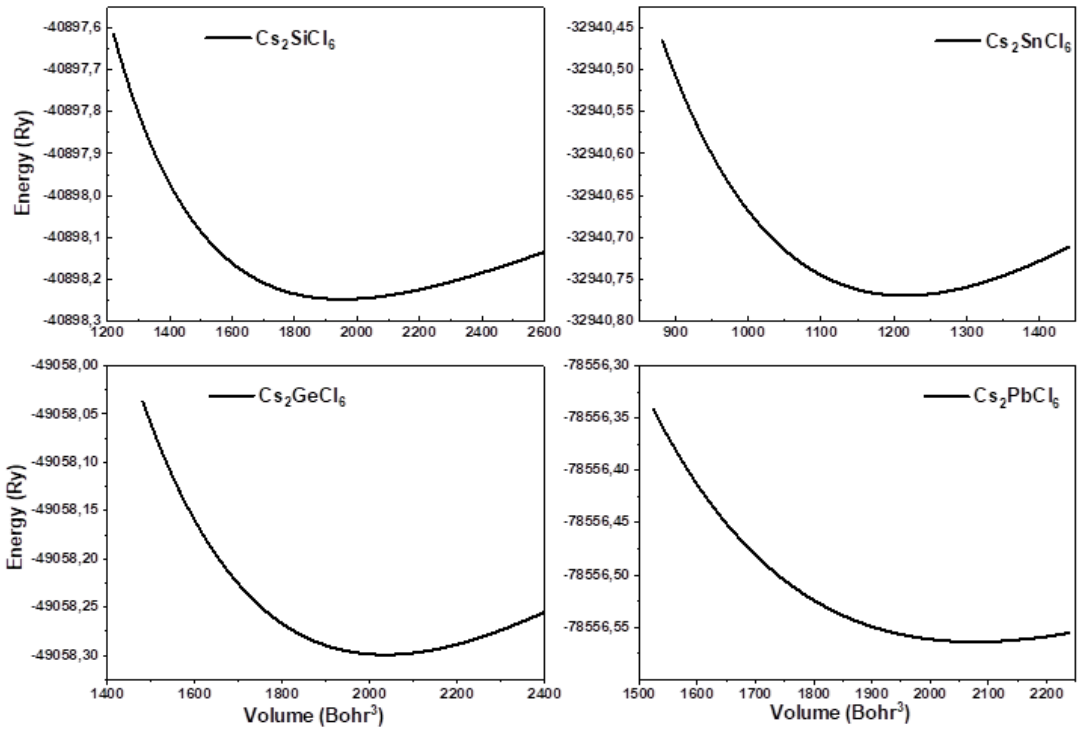

Fig. III. 2. Variation of energy as a function of volume for Cs_2MCl_6 (M = Si, Sn, Ge and Pb) double perovskites.

The lattice constant increases proportionally with atomic sizes. Regarding the bulk modulus and its pressure derivative a negligible deviation was observed for the results extracted in the papers [75, 76], The rest of the quantities not referred to in references are considered future references

Table III. 2. The lattice constant values *a* (Å), the bulk modulus B (GPa) and its derivative pressure B', as well as the minimum energy E_0 (Ry) for Cs_2MCl_6 (M = Si, Sn, Ge and Pb) compounds.

	a_0 (Å)	B (GPa)	B'	E_0 (Ry)
Cs_2SiCl_6	8.955	55.699	4.546	-32940.769
Cs_2GeCl_6	10.490	27.514	5.035	-40898.248
Cs_2SnCl_6				
This work	10.638	27.595	5.018	-49058.299
Experiment	10.3562 [6]	32.21 [8]		
other	10.646 [7]	33.175 [7]	4.9637 [9]	-49058.332 [9]
Cs_2PbCl_6				
This work	10.712	23.594	5.365	-78556.564
Experiment				
other	10.23 [8]			

III.4. Electronic properties

III.4.1 band structure and density of state

The electronic configuration of Si, Sn, Ge, Pb, Cl and Cs are [Ar] $3s^2$ $3p^2$, [Kr] $4d^{10}$ $5s^2$ $5p^2$, [Ne] $3d^{10}$ $4s^2$ $4p^2$, [Xe] $6s^2 4f^{14} 5d^{10}$ $6p^2$, [Ne] $3s^2$ $3p^5$ and [Xe] $6s^1$.

The electronic band structures and densities of states of Cs_2MCl_6 (M = Si, Sn, Ge and Pb) double perovskites calculated using GGA approximation are depicted in Figs. IV. 3 and 4, along the high symmetry lines of the Brillouin zone, where the Fermi level is set to 0 eV.

It is noted that the profiles of the bands obtained are quite similar. Cs_2SiCl_6 and Cs_2GeCl_6 show an indirect W-Γ band gap, while the others have Γ -Γ direct band gap character.

For all compounds, the part located beyond the Fermi level, where the contribution is due to Cl atom, the first conduction band is due to Cl atom, the second conduction band is due to Cs and Cl atoms and low contribution of M (Si, Ge, Sn and Pb) atoms.

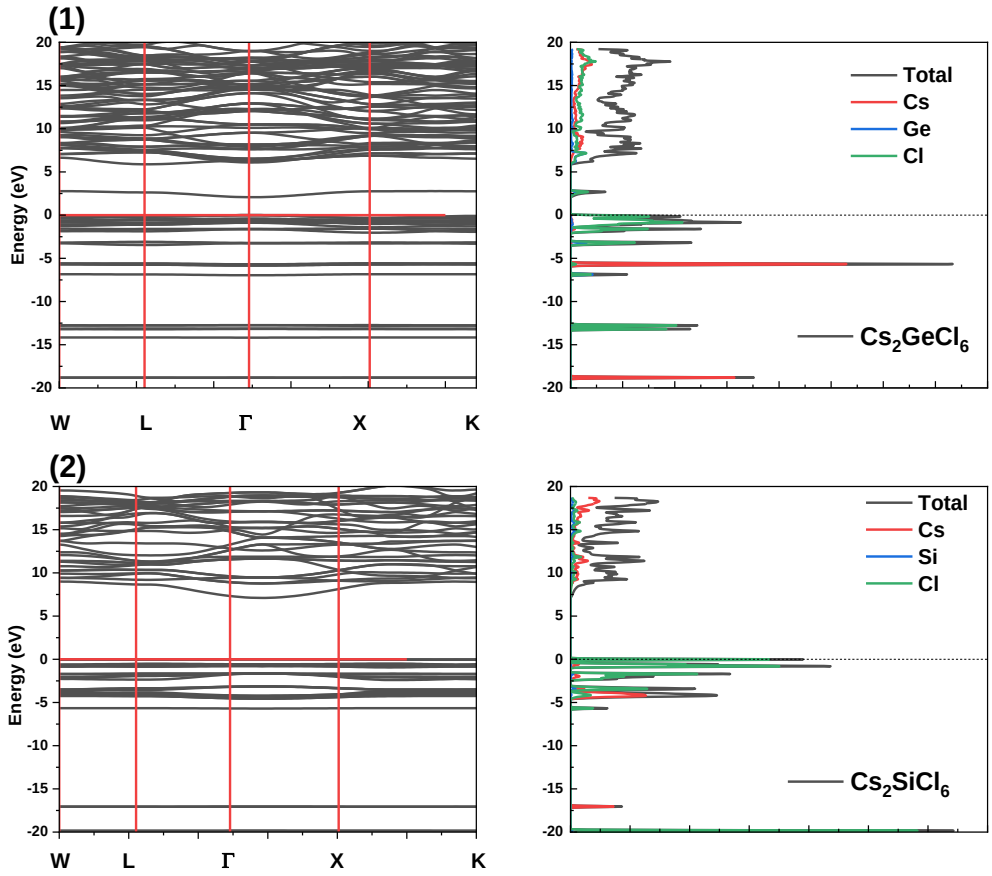

Fig. III.3. (1 and 2). Electronic band structures of Cs_2MCl_6 (M = Si, Ge) using GGA approximation.

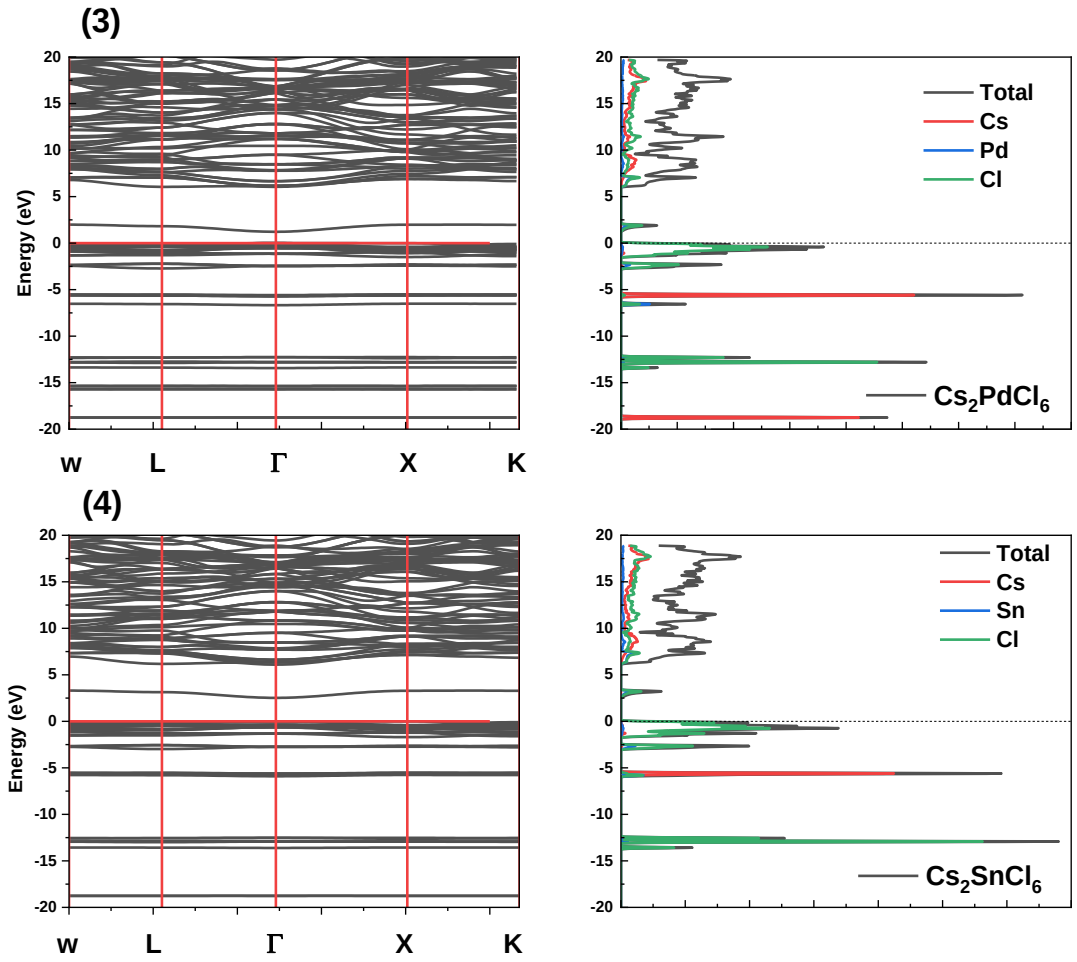

Fig. III. 3. (3 and 4b). Eelectronic band structures of Cs_2MCl_6 (M = Sn, Pd) using GGA approximation.

The calculated fundamental band gap using GGA and mBJ-GGA are listed in Table III. 3, with their theoretical [77] and experimental [78] data. DFT is known to underestimate the values of band gap due to the uncertainty in determining the excited states energies and the GGA-mBJ gives band gap closer to the experimental value.

In general, we obtained closer values compared to those calculated previously by R. Zeng [78] and M. Klintenberg [77].

Table III. 3. Band gap of Cs_2MCl_6 (M = Si, Ge, Sn and Pb) using GGA and GGA-mBJ.

	GGA	mBJ	Experement	Other GGA calculation
Cs_2SiCl_6	7.10229	10.59513		
Cs_2GeCl_6	2.07489	3.50473		
Cs_2SnCl_6	2.52440	3.86302	3.9 [71]	
Cs_2PbCl_6	1.21649	2.18149		1.36 [72]

III.5. Optical behavior

Optical characterization provides a picture of a material's use in optoelectronic devices. The real part of the dielectric constant provides information on polarization and dispersion of light, while the imaginary component represents its absorption when the frequency exceeds a threshold.

The real part of the dielectric function as a function of photon energy is displayed in Fig. III 4. The dielectric function is treated by their real $\varepsilon_1(\omega)$ and imaginary $\varepsilon_2(\omega)$ parts, which respectively explains the electronic polarizability of a material and provides information about the absorption of a crystal.

The static dielectric constant for Cs_2SiCl_6, Cs_2GeCl_6, Cs_2SnCl_6 and Cs_2PbCl_6 using GGA approximation 1.5, 2.8, 2.78 and 3.5 for Cs_2MCl_6 (M = Si, Ge, Sn and Pb). It reaches a maximum value of 2.5, 5.5, 5.3 and 5.4 at 10 eV, 5.8 eV, 5.8 eV and 4 eV.

The dielectric constant of a material is a measure of its ability to store electrical energy. Dielectric constant is a characteristic of a material to reduce the electrostatic force acting between two charges.

The real part becomes negative for an energy in the range 12 to 14 eV. This can be explained by the fact that the dielectric function has an excited field in opposite direction to the external field. This phenomenon occurs when the frequency of the external field is too low. We cannot compare these results due to the absence of experimental data in the literature.

The low values of the static dielectric constant for $Cs_2(Si, Ge, Sn, Pb)Cl_6$ are mainly due to the contribution of the valence electrons of their constituents Cl, Si, Ge, Sn, Pb and Cs to the lattice dynamic properties at energies lower to the band gap. The real dielectric constant of these compounds is smaller in the ultraviolet region.

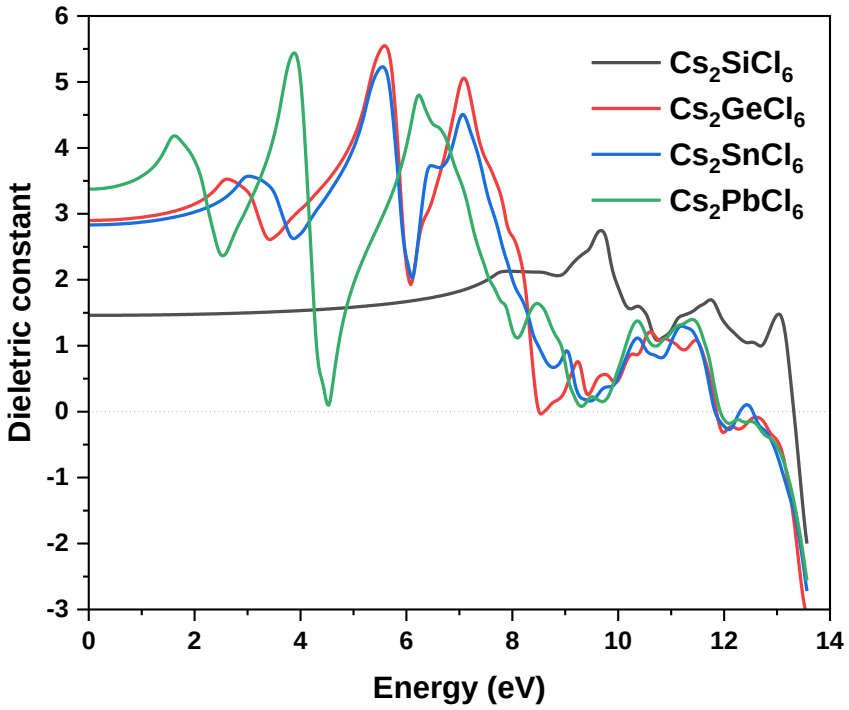

Fig. III. 4. Real part of the dielectric function as a function of photon energy for Cs_2MCl_6 (M = Si, Ge, Sn and Pb) using GGA.

The refractive index of $Cs_2(Si, Ge, Sn, Pb)Cl_6$ is visualized in Fig. III. 5. The refractive index of a material describes the amount of light refracted in a material and depends on the speed of propagation of light in that material, and it is correlated to the optical transition.

The static refractive index of Cs_2SiCl_6, Cs_2GeCl_6 , Cs_2SnCl_6 and Cs_2PbCl_6 is 1.2, 1.65, 1.5 and 1.8. The static refractive index reaches a maximum value of 1.6, 2.3, 2.1 and 2.3 and then rapidly decreases in a linear manner. We note that static refractive index and dielectric constant are connected to the band gap.

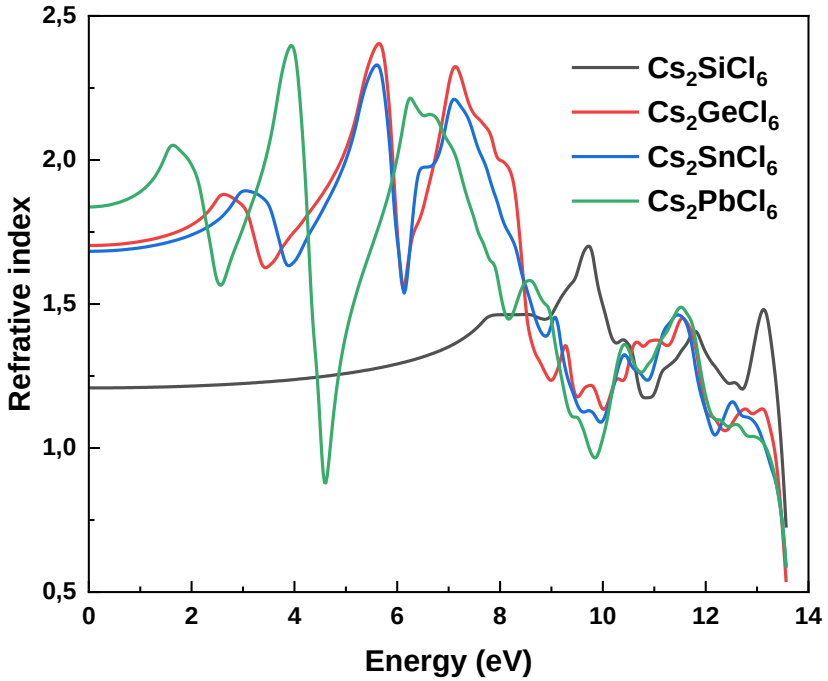

Fig. III. 5. Refractive index as a function of photon energy for Cs_2MCl_6 (M = Si, Ge, Sn and Pb) using GGA.

We trace the absorption diagram in Fig. III. 6. Absorption depends on the energy of the incident photon equal to or greater than the threshold. The thresholds are closer to the calculated band gap and are attributed to the inter-band electronic transitions. Absorption in the visible range is less significant than that in the ultraviolet light. The significant absorption in the ultraviolet region and the adequate band gap advantage these materials for solar cells applications. We report the energy loss spectrum of $Cs_2(Si, Ge, Sn, Pb)Cl_6$ in Fig. III. 7. The loss of energy is due to its transformation from one form to another. The energy loss in $K_2(Se, Sn, Te)Br_6$ is located between 4 eV to 10 eV in the ultraviolet region.

Fig. III. 7 explains the energy loss of fast electrons penetrating the materials under study, and depicts an intense peaks at photon energies at 5eV for Cs_2SiCl_6 and between 9 and 10 eV for Cs_2GeCl_6 , Cs_2SnCl_6 and Cs_2PbCl_6.

These peaks linked to plasma resonance occur when the real dielectric constant is negative, with a rapid reduction in reflectance and the material becomes transparent.

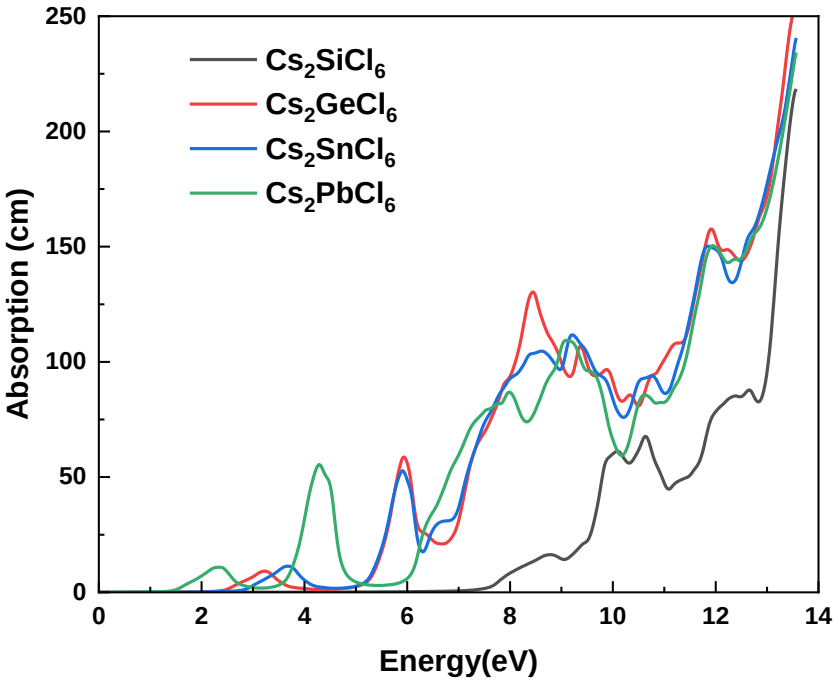

Fig. III. 6. Absorption as a function of photon energy for Cs_2MCl_6 (M = Si, Ge, Sn and Pb) using GGA.

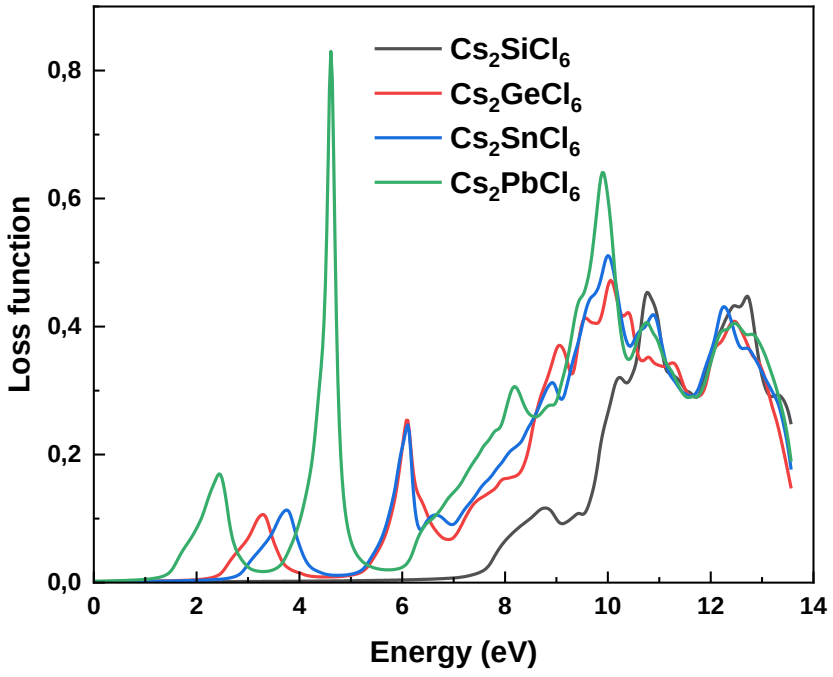

Fig. III. 7. Energy loss a function of photon energy Cs_2MCl_6 (M = Si, Ge, Sn and Pb) using GGA.

III.6. Simulation of Solar Cells based on Cs_2PbCl_6 and Cs_2SiCl_6 semiconductors

III.6.1 Introduction

The solar cell is an electronic component that converts sunlight in electricity in a semiconductor material. The current objective is to achieve a photovoltaic cell with better performance.

Solar cells in thin layers based on Copper, Indium and Gallium Selenide (CIGS) represent the most promising approach to the plan for reducing production costs. The advantage of this material is its easy elaboration, its stability and shows great resistance to radiation [79-80].

III.6.2 The photovoltaic cell

The photovoltaic cell is a basic element in the conversion of radiation solar. Semiconductor materials, particularly silicon and germanium, are the most used. The structure of a solar cell is similar to that of a PN junction [81].

III.6.3 Principle of operation of the photovoltaic cell

The solar cell is an electronic component capable of providing energy electric under illumination. The photovoltaic cell thus constitutes a generator elementary electrical.

The development of solar cells based on **gallium phosphide (GaP)** and **Zinc Oxide (ZnO)** is due to the use of thin film semiconductors [82]. Using metal substrates instead glass constitutes a real additional problem.

III.6.4 Structure of the photovoltaic cell studied

In its most widespread structure, **gallium phosphide GaP** cell is formed of a stack of several materials in thin layers deposited successively on a substrate.

The main elements in the cell are the **gallium phosphide (GaP)** absorber, the buffer layer and the window.

1- The absorber is the most important layer in the photovoltaic cell, because that it absorbs the radiation. The absorber is used from a direct band gap material and a significant absorption coefficient and its conductivity is p-type [83, 84].

2- The buffer layer is an n-type semiconductor located between the absorber and the window [85]. Various materials are used as buffer layers such as **Cs_2SiCl_6**. The buffer layer protects the surface of the absorber [85].

3- The window layer covers the buffer layer. This layer is composed of a deposit of zinc oxide (ZnO).

In this part, we study the solar cell based on **gallium phosphide (GaP)**. The absorber is a p-type semiconductor and constitutes the zone where electron-hole pairs are generated under illumination. The junction is formed with **Cs_2SiCl_6./ ZnO**.

We use a COMSOL simulator. Our work consists of modeling a solar cell based on **gallium phosphide (GaP)**. In our study, we use a solar cell composed of the following heterojunctions: Window (**ZnO**), Buffer (**Cs_2SiCl_6**), **gallium phosphide GaP** (Absorber), is shown in Figure IV. 1.

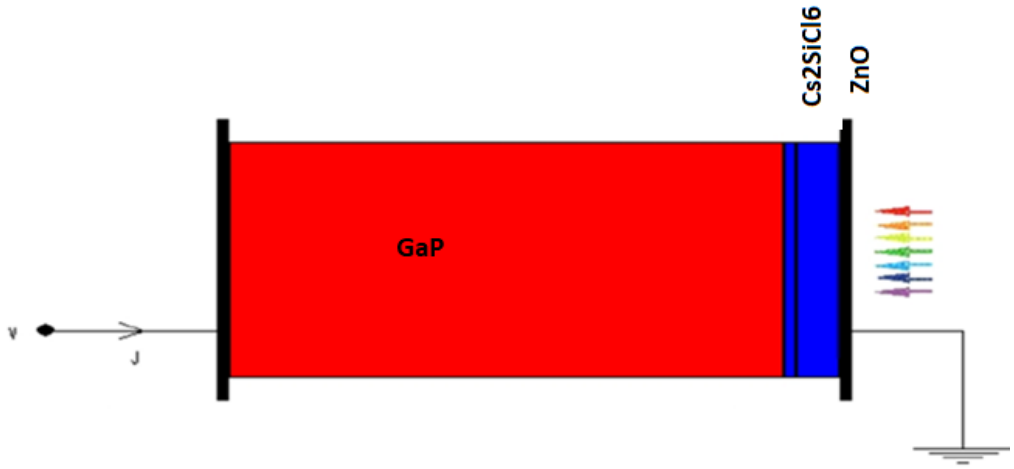

Fig. III. 8. Representation of a solar cell.

We study the effect of voltage and buffer on current for solar cell as shown in Fig. IV 2. We used two buffers such as Cs_2SiCl_6 and Cs_2PbCl_6. It is reported that Cs_2PbCl_6 and Cs_2SiCl_6 buffers give better performance with an operating point of I = 6.5 mA/cm and V = 1.5 V.

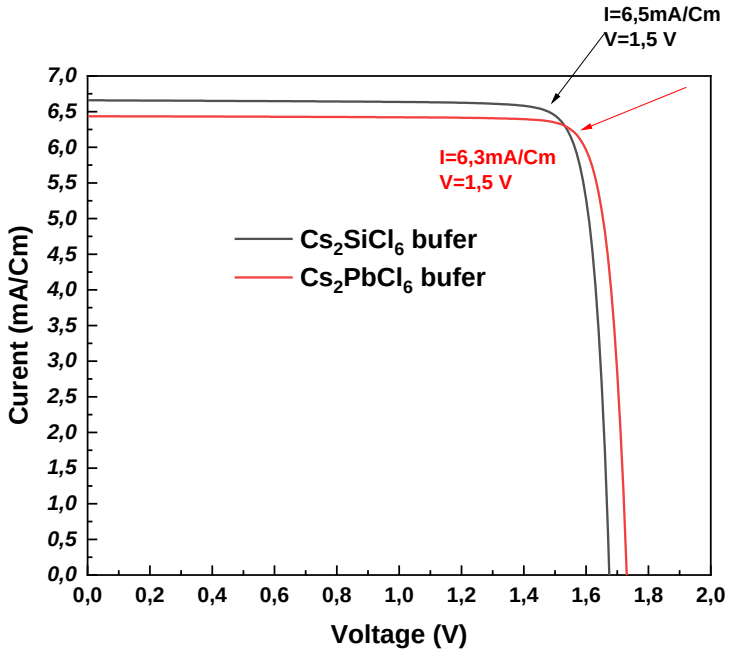

Fig. III. 9. Effect of buffer and voltage on performance of solar cell.

General Conclusion

General Conclusion

The structural, electronic and optical properties of Cs_2MCl_6 (M = Si , Sn, Ge and Pb) semiconductors were studied by the GGA and mb GGA approximation using the full pseudo-potential method and density functional theory (DFT) in the Wien2k code.

The mesh constant, the compressibility modulus and its derivative with respect to the pressure are in agreement with the experimental and theoretical results. Cs_2SiCl_6 and Cs_2GeCl_6 show an indirect W-Γ band gap, while the others have Γ -Γ direct band gap character.

For all compounds, the part located beyond the Fermi level, where the contribution is due to Cl atom, the first conduction band is due to Cl atom, the second conduction band is due to Cs and Cl atoms and low contribution of M (Si, Ge, Sn and Pb) atoms.

The values of the absorption coefficients have adequate and acceptable values in the application of the photovoltaic cell. All the results obtained for Cs_2MCl_6 (M = Si , Sn, Ge and Pb) are in good agreement with those relating to the theoretical and experimental values cited in the literature.

A solar cell based on **gallium phosphide (GaP)** and **Zinc Oxide (ZnO** was produced using the **COMSOL** simulator tool. It is reported that Cs_2PbCl_6 and Cs_2SiCl_6 buffers give better performance with an operating point of I = 6.5 mA/cm and V = 1.5 V.

References

[1]https://www.udel.edu/udaily/2022/may/institute-energy-conversion-photovoltaics-solar-technology/ 2024 – 05 - 20

[2] **Kittel, C., Poumellec, M., Mégy, R., & Dupas, C. (1993).** *Physique de l'état solide*. Dunod.

[3] **Mathieu, H., & Fanet, H. (2009).** *Physique des semiconducteurs et des composants électroniques-6ème édition: Cours et exercices corrigés*. Dunod.

[4] **Souici, A. H., & de Cristallographie, G. (2013).** Physique des Semi-conducteurs. *Polycopié de Cours, Faculté des Sciences Exactes, Université de Béjaia, Algérie*.

[5] **Castagné, R., Duchemin, J. P., & Gloanec, M. (1989).** *Circuits intégrés en arséniure de gallium: physique, technologie et règles de conception*. Masson.

[6] **Laval, S. (1990).** Physique des semiconducteurs III-V. In *Collection de la Société Française d'Optique* (Vol. 1, pp. 35-68). EDP Sciences.

[7] **Ghebouli M A, (2014).** Etude des propriétés des semi-conducteurs CaxMg1-xA (A=S, Se et Te) et MnxCa1-xS par les méthodes ab-initio, Unive De Bordj Bou Arreridj.

[8] **Blakemore, J. S. (1982).** Semiconducting and other major properties of gallium arsenide. *Journal of Applied Physics*, *53*(10), R123-R181.

[9] **Lévy, F. (1995).** *Physique et technologie des semiconducteurs* (Vol. 18). PPUR presses polytechniques.

[10] **P. Dollfus, S. Galdin-Retailleau et A. Bournel, (2013).** "Du cristal au bipolaire", [PDF Document]-FDOCUMENTS

[11] **Zhao, J. (2013).** *Etude théorique d'oxydes nano-structurés multifonctionnels* (Doctoral dissertation, Bordeaux 1).

[12] **Nielsen, O. H., & Martin, R. M. (1985).** Stresses in semiconductors: Ab initio calculations on Si, Ge, and GaAs. *Physical Review B*, *32*(6), 3792.

[13] **Nederveen, C. J., & Van der Wal, C. W. (1967).** A torsion pendulum for the determination of shear modulus and damping around 1 Hz. *Rheologica Acta*, *6*(4), 316-323.

References

[14] **Read, B. E., & Dean, G. D. (1978).** The determination of dynamic properties of polymers and composites. *(No Title)*.

[15] **Iotova, D., Kioussis, N., Blanco, J. R., Lim, S. P., & Wu, R. Q. (1997).** Chemical bonding and elastic constants of Ni-based intermetallics. *Proc. of 1st IAC*, *389*.

[16] **Stiros, S. C., Pirazzoli, P. A., Laborel, J., & Laborel-Deguen, F. (1994).** The 1953 earthquake in Cephalonia (Western Hellenic Arc): coastal uplift and halotectonic faulting. *Geophysical Journal International*, *117*(3), 834-849.

[17] **Hill, R. (1952).** The elastic behaviour of a crystalline aggregate. *Proceedings of the Physical Society. Section A*, *65*(5), 349.

[18] **Voigt, W. (1928).** Lehrbuch der Kristallphysik (Textbook of crystal physics). *BG Teubner, Leipzig und Berlin*.

[19] **Reuss, A., (1929).** "Calculation of the yield point of mixed crystals", Math. Mech. 9, 55.

[20] **Kittel, C. (1983).** Physique de l'état solide, 5ieme édition. *Dunod Université*.

[21] **P Blöchl, P. E., Jepsen, O., & Andersen, O. K. (1994).** Improved tetrahedron method for Brillouin-zone integrations. *Physical Review B*, *49*(23), 16223.

[22] **Hohenberg, P., & Kohn, W. (1964).** Inhomogeneous electron gas. *Physical review*, *136*(3B), B864.

[23] **Kohn, W., & Sham, L. J. (1965).** Self-consistent equations including exchange and correlation effects. *Physical review*, *140*(4A), A1133.

[24] **Dreizler, R. M., & Gross, E. K. (2012).** *Density functional theory: an approach to the quantum many-body problem*. Springer Science & Business Media.

[25] **Sólyom, J. (2007).** *Fundamentals of the Physics of Solids*. Springer-Verlag New York, Inc.

[26] **Rossler, U. (2004).** Solid State Theory: An Introduction. *Heidelberg, Springer-Verlag Berlin Heidelberg, 2004. 336*.

[27] **Born, M. JR. (1927).** Oppenheimer, Ann. Phys.84, 457.

[28] **Cottenier, S. (2002).** Density Functional Theory and the family of (L) APW-methods: a step-by-step introduction. *Instituut voor Kern-en Stralingsfysica, KU Leuven, Belgium*, *4*(0), 41.

References

[29] **Bethe, H. A., & Jackiw, R. W. (1997).** Intermediate quantum mechanics. *Intermediate quantum mechanics*.

[30] **Slater, J. C. (1960).** Quantum theory of atomic structure. *(No Title)*.

[31] **Gaunt, J. A. (1928, April).** A theory of Hartree's atomic fields. In *Mathematical Proceedings of the Cambridge Philosophical Society* (Vol. 24, No. 2, pp. 328-342). Cambridge University Press.

[32] **Allan, G., & Lannoo, M. (1983).** Trends in the cohesive properties of sp bonded elements. *Journal de Physique*, *44*(12), 1355-1363.

[33] **Medkour, Y. (2018).** *Contribution à l'étude des propriétés élastiques des phases M2AX* (Doctoral dissertation, Université de Sétif 1-Ferhat Abbas).

[34] **Thomas, L. H. (1927, January).** The calculation of atomic fields. In *Mathematical proceedings of the Cambridge philosophical society* (Vol. 23, No. 5, pp. 542-548). Cambridge University Press.

[35] **Fermi, E. (1928).** Eine statistische Methode zur Bestimmung einiger Eigenschaften des Atoms und ihre Anwendung auf die Theorie des periodischen Systems der Elemente. *Zeitschrift für Physik*, *48*(1), 73-79.

[36] **Bloch, F. (1928).** Zeitschriftfür Physik 52, 555-600.

[37] **Iabdellaoui, I. (2016).** Étude par les méthodes ab initio les propriétés structurales, électroniques et optiques de V02 en vue de ces applications comme matériau intelligent (Doctoral dissertation, Université de Tlemcen-Abou Bekr Belkaid).

[38] **Kohn, W. (1999).** Nobel Lecture: Electronic structure of matter—wave functions and density functionals. *Reviews of Modern Physics*, *71*(5), 1253.

[39] **Martin, R. M. (2020).** *Electronic structure: basic theory and practical methods*. Cambridge university press.

[40] **Gaunt, J. A. (1928, April).** A theory of Hartree's atomic fields. In *Mathematical Proceedings of the Cambridge Philosophical Society* (Vol. 24, No. 2, pp. 328-342). Cambridge University Press.

[41] **Becke, A. D. (1992).** Density-functional thermochemistry. I. The effect of the exchange-only gradient correction. *The Journal of chemical physics*, *96*(3), 2155-2160.

[42] **Larbi, R. (2020).** "Etude des propriétés structurale et électronique et optique des semi-onducteursCdS et ZnO pour des applications des photovoltaïques" Université Mohamed Boudiaf, M'sila.

[43] **Zeghad, A. (2020).** "Etude des propriétés physiques des semi-onducteursGaX (X=P, As et Sb) par la méthode Ab-initio", Université Mohamed Boudiaf, M'sila (2020).

References

[44] **Qteish, A., & Munoz, A. (2000).** Ab initio study of the phase transformations of ZnSe under high pressure: stability of the cinnabar and SC16 phases. *Journal of Physics: Condensed Matter*, *12*(8), 1705.

[45] **Smelyansky, V. I., & John, S. T. (1995).** Theoretical study on the high-pressure phase transformation in ZnSe. *Physical Review B*, *52*(7), 4658.

[46] **Lakshmi, N., Rao, N. M., Venugopal, R., Reddy, D. R., & Reddy, B. K. (2003).** Formation of mixed phases and mutual chemical analogs in ZnTe–CdS films. *Materials chemistry and physics*, *82*(3), 764-770.

[47] **Khenata, R., Bouhemadou, A., Sahnoun, M., Reshak, A. H., Baltache, H., & Rabah, M. (2006).** Elastic, electronic and optical properties of ZnS, ZnSe and ZnTe under pressure. *Computational Materials Science*, *38*(1), 29-38.

[48] **Ferahtia, S. (2016).** thèse de Doctorat, Université Mohamed Khider, Biskra.

[49] **Kiréev, P. S., & Medvedev, S. V. (1975).** *La physique des semiconducteurs*. Mir.

[50] **Monkhorst, H. J., & Pack, J. D. (1976).** Special points for Brillouin-zone integrations. *Physical review B*, *13*(12), 5188.

[51] **Payne, M. C., Teter, M. P., Allan, D. C., Arias, T. A., & Joannopoulos, A. J. (1992).** Iterative minimization techniques for ab initio total-energy calculations: molecular dynamics and conjugate gradients. *Reviews of modern physics*, *64*(4), 1045.

[52] **Ghebouli M A, (2015).** thèse de Doctorat, Université El bachir El ibrahimi, Bordj Bou Arreridj.

[53] **Phillips, J. C., & Kleinman, L. (1959).** New method for calculating wave functions in crystals and molecules. *Physical Review*, *116*(2), 287.

[54] **Antončík, E. (1959).** Approximate formulation of the orthogonalized plane-wave method. *Journal of Physics and Chemistry of solids*, *10*(4), 314-320.

[55] **Hamann D. R., Schlüter, M. Chiang, C. (1979).** "Norm-ConservingPseudopotentials", Phys. Rev. Lett. 43, 1494.

[56] **Bachelet, G. B., Hamann, D. R., & Schlüter, M. (1982).** Pseudopotentials that work: From H to Pu. *Physical Review B*, *26*(8), 4199.

[57] **Hamann, D. R. (1989).** Generalized norm-conserving pseudopotentials. *Physical Review B*, *40*(5), 2980.

[58] **Slater, J.C. (1937)** *Phys. Rev*. 51 846.

[59] **Herring, C. (1940)** *Phys. Rev*. 57 1169.

[60] **Andersen, O.K. (1975)** *Phys. Rev. B* 12 3060.

[61] **Kanoun, M. B. (2004)** *Thèse de doctorat, université de Tlemcen*.

References

[62] **Koelling D.D. and Arbman G.O., (1975)** *J. Phys. F* 5 2041.

[63] **Vanderbilt, D. (1990).** Soft self-consistent pseudopotentials in a generalized eigenvalue formalism. *Physical review B*, *41*(11), 7892.

[64] **Segall, M. D., Lindan, P. J., Probert, M. A., Pickard, C. J., Hasnip, P. J., Clark, S. J., & Payne, M. C. (2002).** First-principles simulation: ideas, illustrations and the CASTEP code. *Journal of physics: condensed matter*, *14*(11), 2717.

[65] **Clark, S. J., Segall, M. D., Pickard, C. J., Hasnip, P. J., Probert, M. I., Refson, K., & Payne, M. C. (2005).** First principles methods using CASTEP. *Zeitschrift für kristallographie-crystalline materials*, *220*(5-6), 567-570.

[66] **Khuili, M., Ouhammou, A., Fazouan, N., Atmani, E. H., Allaoui, I., Al-Qaisi, S., ... & Bouidmar, R. (2024).** First-principles study of halide double perovskite Cs2SnX6 (X= Cl, Br, I) for solar cell applications. *Modern Physics Letters B*, *38*(01), 2350223.

[67] **Ali, M. A., Alshahrani, T., & Murtaza, G. (2021).** Defective perovskites Cs2SeCl6 and Cs2TeCl6 as novel high temperature potential thermoelectric materials. *Materials Science in Semiconductor Processing*, *127*, 105728.

[68] **P. Blaha, K. Schwarz, G.K.H. Madsen, D. Kvasnicka, J. Luitz, R. Laskowsk, F. Tran,L. Marks, L. (2019).** Marks, Mater. Sci. Eng.

[69] **Anisimov, V. I., & Gunnarsson, O. (1991).** Density-functional calculation of effective Coulomb interactions in metals. *Physical Review B*, *43*(10), 7570.

[70] **Bomaza, A. (2014).** Thèse de Doctorat, Université d'Annaba.

[71] **Brill, T. B., Gearhart, R. C., & Welsh, W. A. (1974).** Crystal structures of M2SnCl6 salts. An analysis of the "crystal field effect" in their nuclear quadrupole resonance and vibrational spectra. *Journal of Magnetic Resonance (1969)*, *13*(1), 27-37.

[72] **Berri, S. (2022).** Thermoelectric properties of A2BCl6: a first principles study. *Journal of Physics and Chemistry of Solids*, *170*, 110940.

[73] **Ullah, R., Ali, M. A., Katubi, K. M., Alsaiari, N. S., Abualnaja, K. M., Verma, A. S., & Murtaza, G. (2022).** Modeling of bulk modulus of A2BX6 cubic crystals (A= K, Cs, Rb, TI, NH4; B= tetravalent cation; X= F, Cl, Br, I) using semi-empirical model. *Inorganic Chemistry Communications*, *139*, 109315.

[74] **Bouferrache, K., Ghebouli, M. A., Ghebouli, B., Habila, M. A., Chihi, T., Fatmi, M., ... & Sillanpaa, M. (2024).** Crystal structure, mechanical, electronic, optical and thermoelectric characteristics of Cs2MCl6 (M= Se, Sn, Te and Ti) cubic double perovskites. *Results in Physics*, *56*, 107138.

References

[75] **Al-Lehyani, I. H. (2021).** A first-principle study of the stability and electronic properties of halide inorganic double perovskite Cs2PbX6 (X= Cl, I) for solar cell application. *Arabian Journal of Chemistry*, *14*(2), 102920.

[76] **Zeng R, Bai K, Wei Q, Chang T, Yan J, Ke B, (2021).** Nano Recherche;14:1551–8.

[77] **Klintenberg, M., Derenzo, S. E., & Weber, M. J. (2002).** A systematic search for new scintillators using electronic structure calculations. In *Nanotech: Technical Proceedings of the 2002 International Conference on Computational Nanoscience and Nanotechnology* (Vol. 2).

[78] **Ullaal HS, Zweibel K, Von Roedern B, (1997).** Proc. 26th IEEE Photovoltaic Specialists Conf., Anaheim, CA, USA, p. 301.

[79] **Yamaguchi, M. (1995).** Radiation resistance of compound semiconductor solar cells. *Journal of applied physics*, *78*(3), 1476-1480.

[80] **Belaidi, S, (2015).** Simulation par Excel d'une cellule solaire conventionnelle en Silicium, Université Abdel Hamid Ibn Badis de Mostaganem,

[81] **Shafarman, W. N., Siebentritt, S., & Stolt, L. (2011).** Cu (InGa) Se2 Solar Cells. *Handbook of photovoltaic science and engineering*, *2*, 546-599.

[82] **Daranfed, O., & Aida, M. S. (2013).** Elaboration et caractérisation de couches absorbantes des cellules solaires en couches minces à base de Cu2ZnSnS4.

[83] **CHADEL, A.** *Optimisation et simulation numérique du profil de la couche absorbante et des différentes couches des cellules photovoltaïques à base de CIGS* (Doctoral dissertation, Université de Tlemcen-Abou Bekr Belkaid).

[84] **Sagna, A. (2016).** *Etude et élaboration par Close-Spaced Vapor Transport (CSVT), d'absorbeurs Cu2ZnSnS4 en couches minces polycristallines destinées à la réalisation de photopiles à faible coût* (Doctoral dissertation, Perpignan).

Abstract

Cs_2MCl_6 (M = Si , Sn, Ge and Pb) semiconductors have important properties, particularly in the manufacturing of optoelectronic devices. The structural, electronic and optical properties of Cs_2MCl_6 (M = Si , Sn, Ge and Pb) compounds were studied. We calculated the constant of the mesh, the modulus of compressibility and its derivative with respect to the pressure. The study of the band structure shows Cs_2SiCl_6 and Cs_2GeCl_6 show an indirect W-Γ band gap, while the others have Γ -Γ direct band gap character. A solar cell based on **gallium phosphide** (**GaP)** and **Zinc Oxide (ZnO** was produced using the **COMSOL** simulator tool. It is reported that Cs_2PbCl_6 and Cs_2SiCl_6 buffers give better performance with an operating point of I = 6.5 mA/cm and V = 1.5 V.

Keywords: Wien2k, DFT, GGA, **Zinc Oxide**, **COMSOL**,

Résumé

Les semi-conducteurs Cs2MCl6 (M = Si, Sn, Ge et Pb) possèdent des propriétés importantes, notamment dans la fabrication de dispositifs optoélectroniques. Les propriétés structurales, électroniques et optiques des composés Cs2MCl6 (M = Si, Sn, Ge et Pb) ont été étudiées. Nous avons calculé la constante du maillage, le module de compressibilité et sa dérivée par rapport à la pression. L'étude de la structure de bande montre que Cs2SiCl6 et Cs2GeCl6 présentent une bande interdite W-Γ indirecte, tandis que les autres ont un caractère de bande interdite directe Γ -Γ. Une cellule solaire à base de phosphure de **gallium (GaP) et d'oxyde de zinc (ZnO)** a été produite à l'aide de l'outil de simulation **COMSOL**. Il est rapporté que les tampons Cs2PbCl6 et Cs2SiCl6 donnent de meilleures performances avec un point de fonctionnement de I = 6,5 mA/cm et V = 1,5 V. .

Mots-clés : Wien2k, DFT, GGA, **Oxyde de Zinc, COMSOL,**

ملخص

تتمتع أشباه الموصلات Cs_2MCl_6 (M = Si وSn وGe وPb) بخصائص مهمة، خاصة في تصنيع الأجهزة الإلكترونية الضوئية. تمت دراسة الخصائص التركيبية والإلكترونية والضوئية لمركبات Cs_2MCl_6 (M = Si, Sn, Ge, Pb). قمنا بحساب ثابت الشبكة ومعامل الانضغاطية ومشتقاتها بالنسبة للضغط. أظهرت دراسة بنية النطاق أن Cs_2SiCl_6 وCs_2GeCl_6 يظهران فجوة نطاقية غير مباشرة W-Γ، في حين أن الآخرين لديهم خاصية فجوة نطاقية مباشرة Γ- Γ. تم دراسة خلية شمسية تعتمد على فوسفيد الغاليوم (GaP) وأكسيد الزنك (ZnO) باستخدام أداة محاكاة COMSOL. يُذكر أن المخازن المؤقتة Cs_2PbCl_6 وCs_2SiCl_6 تعطي أداء أفضل مع نقطة تشغيل I = 6.5 مللي أمبير/سم و V = 1.5 فولت .

الكلمات الرئيسية: Wien2k، DFT، GGA، **أكسيد الزنك**، **COMSOL**،